Stony Brook University

Charmonium in strongly-coupled quark-gluon plasma

A Dissertation Presented

by

Clint Young

to

The Graduate School

in Partial Fulfillment of the Requirements

for the Degree of

Doctor of Philosophy

in

Physics

Stony Brook University

August 2010

Stony Brook University

The Graduate School

Clint Young

We, the dissertation committee for the above candidate for the Doctor of Philosophy degree, hereby recommend acceptance of this dissertation.

Edward Shuryak – Dissertation Advisor
Distinguished Professor, Department of Physics and Astronomy

Clark McGrew – Chairperson of Defense
Associate Professor, Department of Physics and Astronomy

Martin Roček
Professor, Department of Physics and Astronomy

Péter Petreczky
Scientist, Brookhaven National Laboratory

This dissertation is accepted by the Graduate School.

Lawrence Martin
Dean of the Graduate School

Abstract of the Dissertation

Charmonium in strongly-coupled quark-gluon plasma

by

Clint Young

Doctor of Philosophy

in

Physics

Stony Brook University

2010

The heavy quark diffusion coefficient is the subject of a great deal of theoretical interest, with both phenomenology and AdS/CFT results pointing towards this transport coefficient being small in comparison to leading-order perturbative results. The heavy quark-antiquark bound state has been modeled with a Langevin equation that takes into account this small diffusion coefficient, as well as the interaction between the quarks in this pair. It was found that both the survival of J/ψ particles in the most central collisions at the RHIC, and the thermalization of the relative abundances of charmonium states, can be explained with this model, where the destruction of quarkonium due to diffusion remains incomplete over the relevant timescales. Finally, this classical approach is replaced with a path integral which describes quarkonium as an open quantum system, so that comparisons can be made between this model and the results from lattice QCD simulations for certain quarkonium correlation functions.

I must thank, first of all, my parents.

Contents

List of Figures

Acknowledgements

I would not be getting this Ph.D. if not for the support of very many people, so let me try acknowledging them all now:

First of all, I would like to thank the people in the Nuclear Theory Group at Stony Brook. Edward Shuryak has been my adviser for almost four years now and is a constant and energetic source of ideas. Derek Teaney has provided a great deal of help to me: from providing the fp.exe computer code for simulating charm quarks to answering all kinds of questions along the way. Gerald Brown made the NTG an inviting place when I began working there, and together with Tom Kuo, Jacobus Verbaarschot, and Ismail Zahed provided some helpful ideas at our group lunches. Finally, Diane Aveni keeps everything running smoothly and has always been very helpful.

I am also thankful to the Physics and Astronomy Department at Stony Brook. The professors who taught the core courses, as well as those who taught advanced topics, did excellent jobs. I am especially thankful to the people in the main office, and to Patricia Peiliker, who helped me with the rules of the Graduate School concerning the thesis requirement and without whom, I might very well not be graduating on time!

I owe thanks to my fellow graduate students. I also need to acknowledge two former students, now successful postdocs: Kevin Dusling and Shu Lin, whose discussions with me about physics I am starting to miss.

Before Stony Brook, I have had many excellent teachers, who understood the importance of their jobs and took them seriously. The Mathematics and the Physics Departments at SUNY Binghamton had excellent teachers who gave students opportunities for study and research that I greatly appreciate and made post-graduate work in physics possible for me.

Finally, I have been blessed with very good friends and family, however I am afraid that I might leave people off if I started naming them out. To put them in groups: they are my friends from Yonkers, SUNY Binghamton, Pinecrest, and Stony Brook. I must specifically thank James O'Dwyer and the O'Dwyer family. I love Daisy! Also, I must specifically thank Doug Broege and the Broege family. Finally, my aunts, uncles, cousins, and brothers have always

been nothing but supportive and very patient with my missing important events because of my work, and I must thank them here for that.

Chapter 1

Introduction

It has been known for almost 40 years that quantum chromodynamics describes strong interactions. $SU(N)$ gauge theories are conformally invariant classically, but this symmetry is broken quantum-mechanically. Unlike quantum electrodynamics, the degrees of freedom of the QCD Lagrangian (quark and gluon fields) do not match up with the physical spectrum of the theory at zero temperature (hadrons). Even the naive "perturbative" vacuum, the Fock state with gluon and quark numbers equal to zero, is unstable due to the self-interaction of the gluon field, making this state a poor approximation of the physical vacuum, which counter-intuitively, has both lower energy and significantly more complicated structure. The physical vacuum consists of objects which cannot be described perturbatively in the coupling constant: solutions which spontaneously break chiral symmetry (instantons) [1] and perhaps also objects which carry magnetic charge [2]. The gluonic sector of the theory, which is just the field strength for an $SU(3)$ gauge field squared, has an additional parameter quantum-mechanically, Λ_{QCD}, a mass scale below which many perturbative approaches are doomed.

The situation is simplified for hadrons consisting of heavy quarks. In the Standard Model, some quarks are unnaturally heavier than others. The charm quark has a mass of approximately 1.3 GeV, making it significantly heavier than the next highest mass quark, the strange quark (70-130 MeV) [3]. This high mass makes the charm quark essentially a static probe of QCD, and describable with first-quantized techniques such as potential models [4–6]. The Cornell potential has both perturbative behavior at short distances (a Coulomb term) and confining behavior at long distances (a linear term), capturing the physics of running coupling in a simple way. These potential models are remarkably successful at describing the spectrum of charmonium at zero temperature, better than one might even initially suspect considering the relatively small separation of the charm quark mass from Λ_{QCD}.

The heavy-ion program at the Relativistic Heavy-Ion Collider (RHIC) differs from particle physics accelerator experiments in that the goal is not to examine any theory's matrix elements at some new energy range, but instead to examine the well-known theory of QCD at new, high temperatures, where changes in the behavior of the underlying quark and gluonic degrees of freedom for timescales on the order of 10 fm/c are expected. One must ask: how will changing the energy density, however significantly, over such a short period of time lead to any observable difference in the final states detected in such collisions? The charged particle multiplicities scale with the center of mass energy s like $s^{1/4}$, from proton-proton collisions up to the most central collisions at the RHIC, making this observable a poor candidate for discovering any new behavior. Also, radial flow shifts the differential yields in transverse momentum of light hadrons from a thermal distribution back to the distribution one should expect, again, from proton-proton collisions.

The best candidates for detecting a change in behavior over these timescales are radial flow, elliptic flow [7], the thermalization of strangeness [8], jet-quenching [9], and J/ψ suppression [10]. Focusing on the last observable: one might expect that the total yield of J/ψ particles in a heavy-ion collision can be determined by estimating the number of nucleon-nucleon collisions in the heavy-ion collision and multiplying the average yield of J/ψ particles in proton-proton collisions by this estimated number of "binary collisions." This does not turn out to be so: there is a depletion in this yield. This behavior was observed by the NA50 collaboration in lead-lead collisions at $\sqrt{s} = 158A\text{GeV}$: at low centralities, the suppression is consistent with that caused by nuclear absorption in proton-nucleus collisions but past a threshold, there is anomalous suppression which increases with centrality.

Edward Shuryak described how charmonium might undergo disassociation due to the "photo-electric effect" [11]. This early prediction of J/ψ suppression had the strength of being a dynamical treatment of the phenomenon. The earliest estimate anticipated a fairly weak supression of quarkonium. Matsui and Satz [12] examined how the free energy of an infinitely heavy quark-antiquark pair changes with temperature, and stated that above the determined temperature where no bound states should continue to exist, all charmonia would be destroyed. This treatment assumes that changes in the yield are not due to dynamics, but rather are due to changes in the spectrum of charmonium at various temperatures, and the only medium effect considered is the change of a (real) potential describing charmonium due to Debye screening. in this approach, the yield of J/ψ may be predicted by drawing the transverse plane of a heavy-ion collision, determining a contour of this plane on which the temperature is some constant T_c above which charmonium does not form, and

assuming that inside this contour, no J/ψ particles may form, and outside this contour, the J/ψ particle are unaffected. The NA50 experiments, within the context of this model, can be thought of as an experimental measurement of this critical temperature. However, the results from PHENIX cannot be made consistent with this model and with the results of NA50: there is significantly less suppression in gold-gold collisions than had previously been anticipated.

The understanding of the state of matter produced in heavy-ion collisions has shifted from being quarks and gluons in a perturbative vacuum to being strongly interacting matter which is actually best described with the hydrodynamical energy-momentum tensor and an equation of state. With this shift in understanding, the understanding of quarkonium in this medium has also changed. We need to return to the methodology of Shuryak's earlier estimate, where the process of suppression occurs dynamically during the plasma phase of the collision.

Outlining how charmonium dynamics can be made consistent with there being a hydrodynamical phase of QCD is the purpose of this dissertation. The outline for this work is as follows:

Chapter 2 will examine the quarkonium spectrum and dynamics, at both zero and finite temperature. The methods of lattice gauge theory will be summarized, as well as the correlation functions calculated with this technique that are relevant to quarkonium. This will lead to a comparison with potential models, which will demonstrate their success. Next, the real-time behavior of heavy quarks at finite temperature, specifically the the heavy quark diffusion coefficient, will be examined from the thermal field theoretic point of view. From here, the Maldacena conjecture will be summarized and applied both to heavy quark and quarkonium dynamics. This section will conclude with discussion of how these results can be used to describe charm at temperatures above deconfinement.

In Chapter 3, these results will be used in a conjectured model for charmonium above deconfinement, where the dynamics is described with Langevin equations with a potential term describing the quark-antiquark dynamics. Stochastic processes will be summarized, and the case will be made for describing charmonium stochastically. This model will be applied to the evolution of an ensemble of charm quark-antiquark pairs, and it will be shown that for values of the parameters relevant for the RHIC, the final yields of J/ψ evolves on a timescale on the same order as the lifetime of the quark-gluon plasma phase at the RHIC, making the yields determined by the dynamics of charmonium and not merely whether or not bound states exist at these temperatures.

In Chapter 4, this model will be applied to a simulation of the evolution of a large ensemble of charm quark and antiquark pairs, whose momenta are

determined with PYTHIA event generation and whose evolution is integrated with a 2+1-dimensional hydrodynamical simulation of the quark-gluon plasma phase of gold-gold collisions at the RHIC. Heavy-ion collisions will be reviewed; specifically, the evidence for the hydrodynamical description at the RHIC will be discussed, as well as some basics of hydrodynamical simulation. Recombinant production of J/ψ particles in heavy-ion collisions will contribute also to the overall yields. The plot of the anomalous suppression versus number of participants in this model will finally be shown, compared with the results from PHENIX, and discussed.

Chapter 5 will show how stochastic dynamics can be achieved in a system where a few heavy degrees of freedom interact with a large number of light degrees of freedom (an "open system"). The calculations involving this system will be done with path integrals, in the same way as was done by Caldeira and Leggett in 1983 except that the focus here will be on propagators in imaginary time. The purpose of this will be to move in a direction where the Langevin model can be compared with quarkonium correlation functions now being calculated using lattice QCD.

Finally in the Conclusions, some final arguments will be made for treating the evolution of charm and charmonium in heavy-ion collisions dynamically, without resorting to any kind of analysis of the spectrum. I will suggest how progress might be made in understanding charmonium above deconfinement; specifically, how models for charmonium in heavy-ion collisions could be compared with the results from a better-controlled tool: correlation functions calculated using lattice QCD.

Chapter 2

Heavy quark and quarkonium dynamics

This chapter discusses the dynamics of heavy quarks above deconfinement, as well as static and dynamical quantities related to quarkonium. In Section 2.1, heavy quark diffusion is examined using thermal field-theoretic techniques, the AdS/CFT correspondence, lattice QCD, and the phenomenology of charmed mesons at the RHIC. In Section 2.2, results from lattice QCD for the correlation function of two Wilson lines are presented, as well as the relationship between these results and the best potential for describing charmonium phenomenologically. Finally, in Section 2.3, the results of an AdS/CFT calculation modeling quarkonium are shown, and how best to model charm quark pairs is discussed.

2.1 The heavy quark diffusion coefficient

The momentum diffusion coefficient is simply the scattering rate averaged with the momentum transferred squared:

$$3\kappa = \int d^3q |\boldsymbol{q}|^2 \frac{d^3\Gamma(\boldsymbol{q}, T)}{dq^3} \tag{2.1}$$

One might ask: the fundamental theory behind the strong interaction is known, so why not simply calculate this rate to a very high order in perturbation theory, use it to calculate the momentum diffusion coefficient, and then move on? Besides the fact that QCD has many properties which are not analytic in the coupling constant and are therefore inaccessible from perturbation theory, the additional problem is that real-time correlation functions in QCD, even at temperatures above deconfinement, are sensitive to the difficult physics

on the soft "electric scale" $q \sim gT$. Hard thermal loops modify the gluon propagators at all orders, and whenever one wishes to improve the calculation to the next highest order, one must include not only higher order diagrams with the same number of external legs, but also diagrams with a greater number of scatters (representing the interference of multiple scatterings in a short amount of time), as well as the corrections to the previous diagrams due to Debye screening's effect at the next order. This makes even the NLO calculation difficult, and resummation nothing but a faint hope at this point in time.

2.1.1 NLO calculation of 3κ

The NLO calculation of the momentum diffusion by Simon-Carot and Moore [13] is an impressive accomplishment. Any transport coefficient, because of its dependence on the correlation functions of products of operators at unequal times, will be sensitive to the "soft" scale, and also in the case of QCD, overlapping scatterings, leading to great difficulty in reaching higher orders of g_s. Using HTL effective theory, these authors found the NLO result to be

$$3\kappa = 16\pi\alpha_s^2 T^3 \left(-\ln g_s + 0.07428 + 1.9026 g_s\right). \tag{2.2}$$

It is instructive at this point to examine a plot of this result as a function of g_s, shown in Figure 2.1. As can be seen, the convergence from leading-order to next-to-leading order is quite poor for all but the smallest values of g_s.

2.1.2 Diffusion in strongly-coupled $\mathcal{N} = 4$ Super Yang-Mills theory

Some time ago now, Maldacena considered a stack of many $D3$-branes and considered the low energy limit of this system's Hilbert space, and found a duality between $\mathcal{N} = 4$ supersymmetric gauge theory in four dimensions and Type IIB supergravity in an AdS_5 background [14]. Subsequently, Witten elaborated this correspondence; specifically, he noted how correlation functions in the conformal field theory relate to the supergravity action, and how the finite-temperature theory relates to the AdS_5 black hole background [15]. This gauge/gravity duality is important in that it relates easy string theory calculations to difficult quantum field theory calculations, independent from any assertions of the validity of string theory as a theory of nature.

This correspondence can be used to calculate the analogue of heavy quark diffusion in $\mathcal{N} = 4$ SYM theory. A very heavy probe of the conformal field theory is dual to an open string with one endpoint terminating on a "probe brane" far from the black brane and the other end of the string passing through

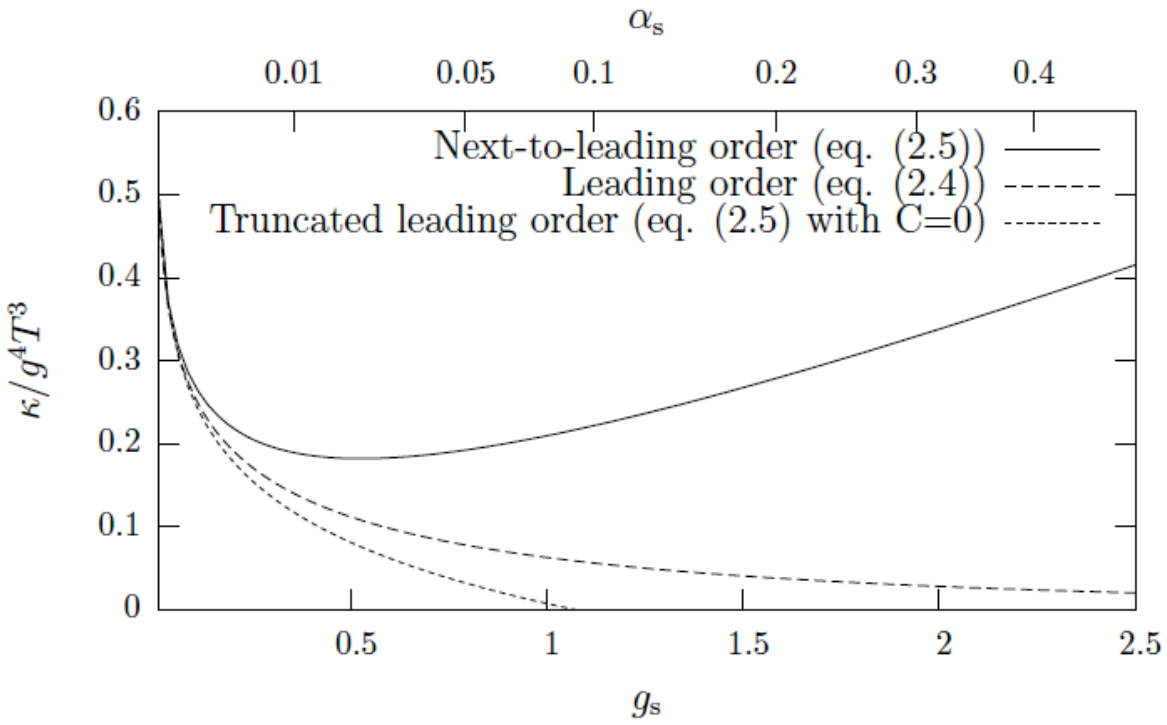

Figure 2.1: The result from [13], compared with the LO result

the horizon and terminating on the black brane. The drag force is related to the energy loss of a moving string: Gubser's calculation of the drag force involved determining the trailing string solution where the endpoint on the probe brane moved at some constant velocity, and then determining the rate of energy transfer from the string to the black brane [16]. Casalderrey-Solana and Teaney determined the diffusion coefficient for a static quark by examining how the string vibrates in AdS_5 and using the fluctuation-dissipation theorem [17]. These results are related through the Einstein relation between momentum diffusion and drag, which will be discussed in Chapter 3.

The result for the momentum diffusion coefficient is

$$3\kappa = \pi\sqrt{\lambda}T^3, \tag{2.3}$$

$\lambda = g_s^2 N_c$. First of all, this is clearly inaccessible with conventional perturbative methods at small values of λ, since the function is not analytic there. Second of all, for $g_s \leq 1$, this result is significantly larger than the result for momentum diffusion at NLO.

2.1.3 Heavy quark diffusion and RHIC phenomenology

The spectrum of D and $\bar{D}$ mesons from gold-gold collisions at the RHIC has been measured with statistics higher by about 2 orders of magnitude than the statistics of charmonium measurements [18]. If diffusive effects are significant to charmonium, then surely they are significant for these charmed mesons, and would have an effect on this spectrum. Moore and Teaney simulated charm in a hydrodynamical simulation as being described by a Langevin equation, sensitive to the flow and temperature of the underlying medium [19]. In this way, the diffusion coefficient might be determined phenomenologically.

Theoretical and experimental results are shown in Figure 2.2. Notice specifically how the results of Moore and Teaney from [19] compare with the PHENIX analysis. None of the various values of the diffusion coefficient lead to convincing agreement with the data for R_{AA}, especially for the lower values of p_T. This is likely due to cold nuclear matter effects, which cause the initial distribution of charm from nucleus-nucleus collisions (before any evolution of these distributions in the medium) to differ substantially from the distributions in proton-proton collisions. Because this R_{AA} is a ratio where the denominator, $N_{coll}dN_{init}/p_T dp_T$, is not well-known, the quality of the theoretical result suffers. However, the elliptic flow (which is an effect entirely absent from proton-proton collisions, due to nearly perfect azimuthal symmetry) is not such a ratio, and only depends on the final distributions of the charm quarks in momentum space. One should expect the results of Moore

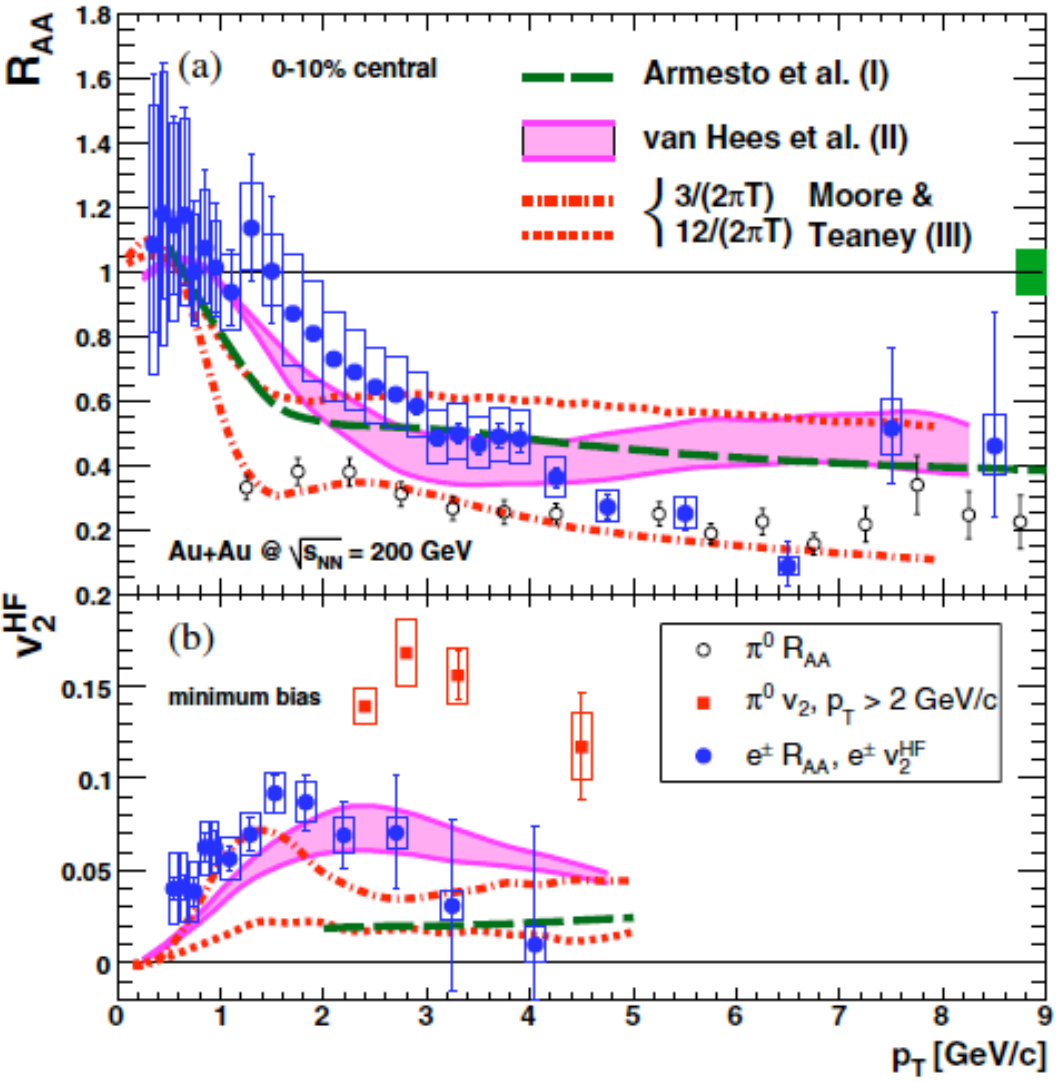

Figure 2.2: Theoretical and experimental results for charm $R_{AA}(p_T)$ and $v_2(p_T)$ compared, from [18].

and Teaney to have greater success here, and indeed, for $2\pi TD_c = 3.0$, there is excellent agreement with the PHENIX results here.

Phenomenology also suggests a very small estimate for the spatial diffusion coefficient, or conversely, a very large momentum diffusion coefficient. The estimate argued here is the smallest estimate for spatial diffusion yet.

2.1.4 Heavy quark diffusion and lattice QCD correlation functions

Using lattice QCD [20], various correlation functions relevant to heavy quarks and quarkonium can be calculated in imaginary time. While it remains difficult work to extract real-time spectral functions from these Euclidean correlation functions, it might not be so difficult to "meet the lattice gauge theorist on the lattice", rather than having the lattice gauge theorists attempt to meet the nuclear theorists in real time. In other words, the effect of various dynamical quantities on imaginary-time correlation functions should be calculated and compared with lattice results, with attention paid to precision and also to which quantities have little effect.

Petreczky and Teaney worked with this philosophy when they examined the effect of diffusion on the Euclidean density-density and current-current correlation functions for single heavy quarks [21]. These Euclidean correlators were found to have a dependence on the spectral function for these currents at small frequencies, and by examining how small fluctuations in density propagate when the heavy quarks obey a Langevin equation, these low-energy contributions can be determined up to a dependence on the diffusion coefficient. They suggested taking the difference between Euclidean correlators calculated on the lattice for two small values of the chemical potential, which should remove the dependence on anything other than the diffusive contribution, which is shown for different temperatures in Figure 2.3.

Lattice QCD remains the most controlled setting for examining QCD. There has been focus lately on taking lattice results and attempting to extract real-time dynamics using Bayesian methods, often with limited results. It may make more sense of the makers of various models instead to make predictions for the Euclidean correlators and compare directly with lattice results. Chapter 4 will focus on how diffusion might affect quarkonium correlators, and how models might be compared with these lattice quarkonium correlators.

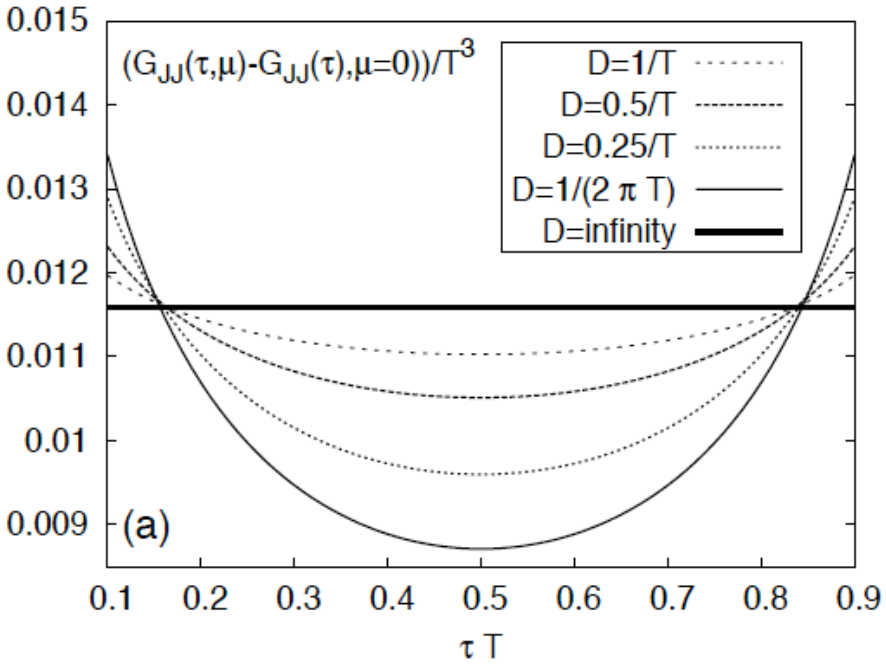

Figure 2.3: The difference between the Euclidean correlators at different chemical potentials, from [21].

2.2 The heavy quark-antiquark potential in the singlet channel

In the case of the heavy quark diffusion coefficient, the best insights came from effective theories, phenomenology, and gauge-gravity duality. Lattice QCD, while being closest to calculations using the original QCD Lagrangian, fails in providing much help in determining the diffusion coefficient, or any other transport coefficient, up until now. However, for the heavy quark-antiquark free energy, which is related to correlation functions of operators at equal times, simulations in Euclidean time offer the hope of precise measurement. In fact, lattice QCD is not only the best tool for measuring this potential, it is the only one of any phenomenological use; effective theories are only useful at short length scales far below the typical radii of quarkonium states, and $\mathcal{N} = 4$ super Yang-Mills theory lacks the conformal symmetry breaking which exists in these potentials.

From the earliest days of research in lattice QCD, effort has been placed in determining the heavy quark-antiquark potential. For the purpose of this work, let us focus on the work of Kaczmarek et al. [22], which concentrates on the potential in temperature ranges of our current interest. The quantity calculated is $\mathcal{Z} = \left\langle \mathrm{tr} L_{\mathbf{x}} \mathrm{tr} L_{\mathbf{y}}^{\dagger} \right\rangle$, which is related to the free energy by $F(|\mathbf{x} - \mathbf{y}|) = -\ln \mathcal{Z}/\beta$. The results of these simulations, as well as an attempt at fitting these results, are shown in Figure 2.4.

Note how difficult it is to fit the results from the lattice to some functional form. Some previous authors fitted the results for each temperature independently to some functional form, then fitted each parameter across all temperatures to another form, quoting the result for this final fit, but only displaying in their plots the results of the independent fits. If they showed instead the result of their best fit for these functions across all temperatures, there would be far poorer agreement between the lattice results and the fit. Here, the lattice results were fitted, *simultaneously across all temperatures and quark separations*, to the functional form

$$V(r,T) = -\alpha \frac{e^{-\mu(T) r^2}}{r} + \sigma r e^{-\mu(T) r^2} + C(T)(1 - e^{-\mu(T) r^2}). \tag{2.4}$$

It would be interesting to find a function which truly fits the lattice results, across all temperatures and quark separations, to a statistically reasonable value for χ^2. This function might provide insight into the structure of the QCD vacuum.

The classical Boltzmann factor $\exp(-U(r)/T)$ for a Coulomb potential leads to a spatial distribution where the probability for small separations is

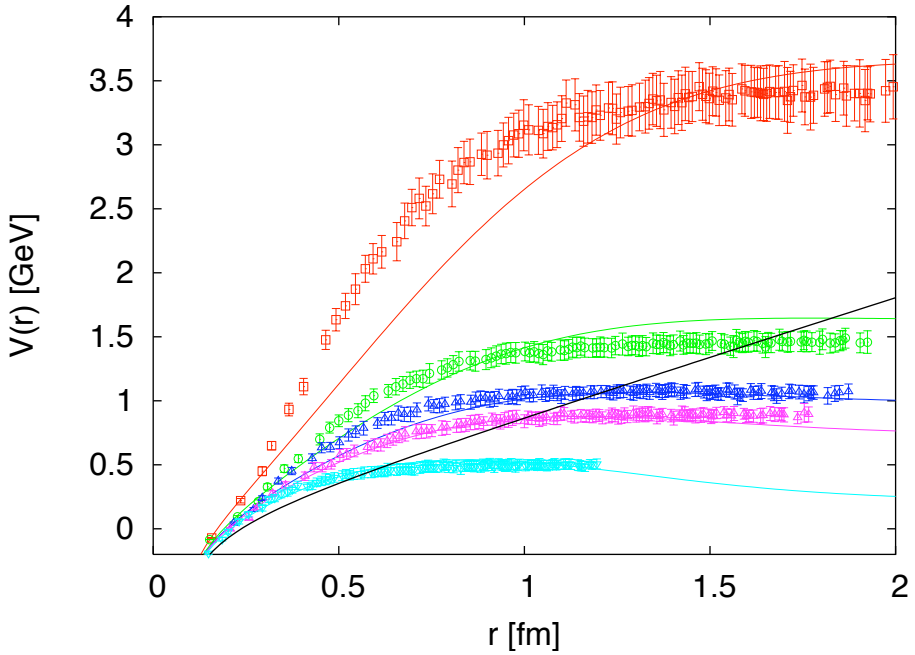

Figure 2.4: The color singlet heavy quark-antiquark potential as determined in [22], calculated at temperatures (from top to bottom) T/T_c=1.02, 1.07, 1.13, 1.18, and 1.64

divergent. This would doom any classical simulation of particles interacting according to this potential. In [24], the diagonal terms of the quantum-mechanical density matrix are calculated, and using the definition

$$\rho(\mathbf{r}, \mathbf{r}, \beta) \propto \exp(-\beta U_{\text{eff}}(\mathbf{r}), \tag{2.5}$$

and effective potential is defined and determined for the lattice potential. This effective potential is necessary for classical simulations of a dilute gas of heavy quasiparticles that form a fundamental representation of the gauge group.

At zero temperature, the heavy quark-antiquark potential, when substituted into the Schrödinger equation, yields an energy spectrum which agrees well with the observed spectrum of charmonium. However, at finite temperature, there are several thermodynamic potentials, with each appropriate only for a specific situation. The potential discussed above, the Helmholtz free energy F, describes the energy of two static quarks in thermal equilibrium with its environment; it is the energy required to create this pair assuming the heat available from the surrounding environment is used. The other potential, the internal energy U, describes the amount of energy required to create the sys-

tem assuming no heat is exchanged with the environment. These potentials are related through a Legendre transformation:

$$F = U - S\frac{dU}{dS} = U - TS. \tag{2.6}$$

The earliest considerations of J/ψ particles above deconfinement worked with the Helmholtz free energy as the potential describing the spectrum. Shuryak and Zahed argued that the timescales relevant to charmonium are short compared with the relaxation time to thermal equilibrium, making the internal energy the relevant potential [25].

2.2.1 Which potential works best? Comparing potential models to quarkonium correlators

The quarkonium correlation function in the vector channel,

$$G(\tau) = \int d^3x \left\langle J_\mu(\mathbf{x},\tau) J^\mu(\mathbf{0},0)\right\rangle, \tag{2.7}$$

where $J^\mu(\mathbf{x},\tau) = \bar{\psi}(\mathbf{x},\tau)\gamma^\mu\psi(\mathbf{x},\tau)$, has been calculated on the lattice above deconfinement [26]. These correlation functions have also been calculated in the scalar, pseudovector, and pseudoscalar channels. Potential models for quarkonium can then be compared with these numerical results, and it was found that the quarkonium correlators can be described with a potential which is screened to the point where not even the J/ψ state exists in the spectrum [27].

In some sense, these lattice quarkonium correlation functions are the best-controlled setting for examining quarkonium starting with the first principles of QCD, and any comparison with these results needs to be taken seriously. However, as was argued in the previous section, the interaction of heavy quarks with light degrees of freedom, parameterized by the momentum diffusion coefficient, cannot yet be ruled out in terms of having a significant effect on quarkonium correlation functions. This effect might render the conclusions of potential models more ambiguous than previously thought. For the remainder of this dissertation, two extremes will be considered when discussing the dynamics of quarkonium: the extreme where the tight-binding internal energy is used as the potential, and the extreme where the potential is set to zero. Also in Chapter 4, the effect of momentum diffusion on Euclidean correlation functions will be considered.

2.3 A grain of salt: dipoles in strongly-coupled $\mathcal{N} = 4$ Super Yang-Mills theory

At this point, single heavy quarks were shown to interact significantly with the medium at finite temperature, and, lattice QCD results for the heavy quark-antiquark potential were found to be modified with temperature and to persist allowing bound states past T_c. The next step is clearly to attempt modeling charmonium dynamics above deconfinement as involving both this diffusive interaction and this potential. Indeed, the remainder of this dissertation will focus on a Langevin-with-interaction model for charmonium in heavy-ion collisions. However, it is important here to note that quarkonium does not necessarily equal two heavy quarks!

In fact, the earliest AdS/CFT calculation examining quarkonium yielded a result quite different from the results for single heavy quarks. In [28], quarkonium is dual to a string in black hole AdS_5 with both endpoints terminating on the probe $D3$ brane at the boundary. In this model, the only effect of the medium is to cause there to be no solution for a string connecting these endpoints above a critical velocity for the quarkonium, leading to this being called "hot wind" disassociation of quarkonium.

This limit of infinite mass for quarkonium is of course problematic, and in fact, no such speed limit for J/ψ in heavy-ion collisions has ever been observed. However, even after relaxing this infinite binding energy limit, quarkonium dynamics can be quite different from what might be expected. In [29], quarkonium is described with a dipole Langrangian coupled to $\mathcal{N} = 4$ super Yang-MIlls, which is dual to the lowest energy fluctuations on a $D7$ brane imbedded in black hole AdS_5. The coupling constants are related to changes in the mass shift of these fluctuations with temperature, and various field strengths in the field theory can easily be calculated by examining the dilaton and graviton fields. The result is that the momentum diffusion for such a dipole is *suppressed* by a factor of 4 compared with the weak coupling expectation.

The difference between these two previous results, and the model for quarkonium that the previous sections suggest, has an analogy from electrodynamics. When visible light scatters off of water in the atmosphere, it "sees" a gas of dipoles, which leads to the familiar Rayleigh scattering and also to the sky being blue. However if an X-ray were to scatter off of the water molecules, it would see individual electrons, due to the X-ray having a wavelength short in comparison to the Bohr radius. An X-ray could disassociate a water molecule while visible light never would. Similarly, the last two results for quarkonium in AdS_5 work in the "Rayleigh scattering" limit, while in the limit of the "photoelectric effect", the heavy quarks forming quarkonium can be mod-

eled as undergoing independent random kicks from the medium as well as an interaction between the quarks in the pair.

How the binding energy of the quarkonium state compares with the temperature determines which limit is appropriate to use. For the Υ particle, the binding energy is significantly larger than the temperature, meaning that the average thermal quasiparticle, having energy on the order of the temperature, will interact with the Υ as if it were a dipole. The Rayleigh scattering limit may be the most appropriate limit here. However for the J/ψ, the binding energy is actually slightly smaller than the typical temperatures reached in heavy-ion collisions. Perhaps the photoelectric limit is most appropriate here, however the J/ψ is not clearly within one limit or the other.

2.4 Summary

With lattice QCD, the heavy quark-antiquark potential, and Euclidean quarkonium correlation functions, are known quite well at finite temperature. However, the real-time dynamics of quarkonium above deconfinement is not so easily determined. Even which (if any) thermodynamic potential is most appropriate for charmonium spectroscopy is not clear, and what value for the diffusion coefficient is appropriate depends on unequal real-time correlation functions, about which lattice simulation still has little to say.

I have made the case, however, for large momentum diffusion and persisting interaction between heavy quark-antiquark pairs in the color singlet state. In the next chapter, I will show how these considerations can lead to a model for quarkonium above deconfinement, and I will show the implications this model has on heavy-ion collisions.

Chapter 3

Langevin-with-interaction dynamics for quarkonium

Inspired by the separation of scales $p \sim \sqrt{MT} >> T$ for charm quarks in heavy-ion collisions, and by what was learned about quarkonium dynamics from the previous chapter, one should attempt to model charmonium in strongly-coupled quark-gluon plasma as undergoing Brownian motion. In Section 3.1, the Langevin equation is introduced, and some general results concerning this equation in particular and stochastic differential equations in general are reviewed. In Section 3.3, ensembles of $\bar{c}c$ pairs are simulated numerically as undergoing Langevin dynamics, with the parameters based on estimates from analysis of heavy-ion collisions. These results are summarized, and the implications for J/ψ-yields in gold-gold collisions at the RHIC are considered.

3.1 The Langevin equation

The non-relativistic Langevin equation approximates dynamics in the the limit $M >> T$. The particle receives many random kicks over the time it takes for the position of the heavy particle to change significantly, making it a good approximation to model these kicks as uncorrelated:

$$\frac{dp_i}{dt} = -\eta p_i + \xi_i(t), \tag{3.1}$$

where η is the drag coefficient and the random force $\xi_i(t)$ is "white noise": $\langle \xi_i(t)\xi_j(t') \rangle = \kappa\delta_{ij}\delta(t-t')$. The index in the equation can label both the particle and the spatial dimension.

This equation is called a *stochastic* differential equation because it is de-

pendent on a random function $\xi_i(t)$. As such, the motion of a single particle according to this equation is not very meaningful and one would be more interested in the evolution of ensembles of particles described by this equation or in functional integrals over $\xi_i(t)$; later sections will describe when and how this can be done. However, it is not too early to calculate an important expectation value: for a heavy particle starting at rest,

$$\begin{aligned}\langle p_i(t)p_j(t)\rangle &= \int_{-\infty}^{t} dt' \int_{-\infty}^{t} dt'' e^{-\eta(2t-t'-t'')} \left\langle \xi_i(t'\xi_j(t'')\right\rangle \\ &= \frac{\kappa}{2\eta}(1-e^{-2\eta t})\delta_{ij}.\end{aligned}$$

Requiring the expectation value to approach the thermal expectation value $MT\delta_{ij}$ yields the Einstein relation between drag and the white noise:

$$\eta = \frac{\kappa}{2MT}. \tag{3.2}$$

Another important expectation value relates the more familiar concept of spatial diffusion to the coefficients here:

$$\begin{aligned}\left\langle x^2(t)\right\rangle &= \int_0^t dt' dt'' \left\langle v(t')v(t'')\right\rangle \\ &= \frac{\kappa}{2\eta M^2}\int_0^t dt' \int_0^t dt'' \exp(-\eta|t'-t''|) \\ &= \frac{2T}{\eta M}(t-e^{-\eta t}/\eta),\end{aligned} \tag{3.3}$$

where the Einstein relation was used to simplify the last line. Since the usual picture of diffusion as a "random walk" gives the result $\langle x^2(t)\rangle = 2Dt$, the spatial diffusion coefficient is best described as $D = 2T/\eta M$ in the Langevin model for Brownian motion. This answers an important question of intuition. Some people, when they think of increasing the drag coefficient for a particle, imagine the particle getting "stuck" in the fluid and experiencing less spatial diffusion, while other people realize that stronger drag, by the Einstein relation, requires stronger momentum diffusion, and imagine the particles getting stronger kicks and experiencing greater spatial diffusion. The relation between spatial diffusion and the drag coefficient provides an unequivocal answer: drag wins, stronger drag means smaller spatial diffusion.

3.1.1 Evolution of an ensemble in phase space: the Fokker-Planck equation

Consider how the phase space distribution $P(\mathbf{x}, \mathbf{p}, t)$ evolves in time. Elements of the ensemble leave the phase space volume $d^3x d^3p$ with velocity $\mathbf{v}$, and enter and leave the phase space volume due to drag and diffusion in momentum space. Expanding into a Taylor series in changes in velocity, determining the expectation values $\langle(\Delta v(t))^n\rangle$, and neglecting these expectation values past $n = 2$, yields the Fokker-Planck equation [30]:

$$\frac{\partial P}{\partial t} = -\frac{\mathbf{p}}{M} \cdot \nabla_x P + MT\eta \nabla_p \cdot (f_0 \nabla_p \frac{P}{f_0}) + \frac{2T}{M\eta} \nabla_x^2 P, \tag{3.4}$$

where $f_0 = \exp(-\frac{p^2}{2MT})$. In this way, an ensemble of particles, each evolving according to a *stochastic*, *ordinary* differential equation, has a dual description in a six-dimensional phase space, where a probability distribution evolves according to a *deterministic*, *partial* differential equation.

3.1.2 Numerical integration of stochastic differential equations

We want a procedure for numerical integration of the Langevin equation. Whenever one integrates a deterministic equation of motion, the usual procedure is to start with some initial $\mathbf{x}_0$ and $\mathbf{p}_0$, and, moving forward in timesteps Δt, determine the variables from step $n + 1$ from step n using the discretized equations of motion. The precision of the numerical integration is determined by the size of the timestep, with a great deal of work going into more sophisticated versions of the equations of motion so that smaller timesteps can be used in the some situations. However, we not only need to integrate over the real variable t, but also over the *functional variable* $\xi(t)$, the noise term in the Langevin equations. To perform such an integral numerically, the only practical approach is the Monte Carlo technique, where large ensembles of particles are simulated and the noise term is sampled with the help of random number generation. Any expectation value can be averaged over this ensemble, however, the precision is not only determined by the size of Δt, but also the number of elements in the simulated ensemble.

So far, only expectation values for particles undergoing Langevin dynamics have been calculated. Given a noise term $\xi_i(t)$, how would the trajectory of a single particle be determined? In the definition of Langevin dynamics, there are no conditions on differentiability for this noise term, only a condition on its auto-correlation function. This poses a problem of mathematics: how can

the integral for such a function be defined?

We know that over a time scale δt, which is long compared with the correlation time of the random force but short compared with the change of position of the particle, $\langle (\Delta p)^2 \rangle = \kappa \delta t$. Over a timescale Δt much larger than δt but still small enough to obtain a reasonable approximation to the differential equation, the particle receives very many uncorrelated kicks. Here, the central limit theorem applies: the probability for the sum of very many random variables to have a given value is determined by a Gaussian distribution. This is the fact behind the ubiquitousness of the normal distribution: for example, a physics student's final exam grade depends on many random variables (how much that student studied on each day of the semester, etc.), so if the grading of all the students is performed fairly, a "bell curve" should be no surprise.

In order to simulate numerically a large ensemble of particles undergoing Langevin dynamics, the particle's path should be discretized to intervals of length Δt and each particle's path should be integrated with the Euler method, with each particle having a kick randomly selected from a Gaussian distribution with variance $\kappa/\Delta t$.

The mathematical considerations necessary for proper definition of stochastic integrals (Ito's calculus for *adapted* stochastic processes) will not be discussed here: for a sufficiently fine resolution of a physical observable, the observable is not only adapted but also continuous, making the Ito integral unnecessary and the usual Riemann-Stieljes integral sufficient. For all the considerations necessary for defining the Ito integral for adapted stochastic processes, see [31].

3.2 Relativistic Langevin dynamics: multiplicative noise

The Langevin equation has a simple relativistic generalization, where the equations of motion are simply written in the rest frame of the medium [19]:

$$\begin{aligned} \frac{dp_L}{dt} &= -\eta(p) p_L + \xi_L, \\ \frac{dp_T^i}{dt} &= \xi_T^i, \end{aligned} \tag{3.5}$$

where $\eta(p)$ is, in general, a function of momentum, and the noise terms have correlation functions $\left\langle \xi_L^i(t) \xi_L^j(t') \right\rangle = \kappa_L(p) \hat{p}^i \hat{p}^j \delta(t - t')$, $\left\langle \xi_T^i(t) \xi_T^j(t') \right\rangle = \kappa_T(p)(\delta^{ij} - \hat{p}^i \hat{p}^j)\delta(t - t')$, and no nonzero cross-correlations between the lon-

gitudinal and transverse noise terms.

The noise terms are now functions of the coordinates p_L and p_T^i, which leads to an ambiguity in the discretization of the equations. The noise term is dependent on the momentum, which jumps due to the random kicks on which it depends. As outlined in the previous section, our procedure will be to simulate a large ensemble of these particles, discretize in time, and sample the noise terms for each particle from a Gaussian distribution, giving us Monte Carlo integration over a functional variable. When integrating the equations one timestep into the future, what value for the momentum should be used? The Ito discretization uses the current value of the momentum (the value at timestep n):

$$(p^{n+1})^i - (p^n)^i = \left(a^i_{Ito}(\mathbf{p}^n) + \xi^i(\mathbf{p}^n)\right)\Delta t. \tag{3.6}$$

The Ito integral is appropriate for stochastic processes known as "càdlàg", which is a French acronym for "right-continuous, left-limited." In such a situation, it makes sense to make the right-hand side only depend on the previous timestep. This integral makes the most sense in determining the profits of a stocks-trading strategy: you should determine your profits from your current holdings, not the stocks you are going to have at the next moment you trade! The Stratanovich integral represents a numerical discretization much like the Ito discretization except that the next timestep depends on the *mean* value of the momentum over the time between steps n and $n+1$.

For physical stochastic processes, it is not always clear which discretization makes more sense, and because different discretizations can lead to different results, this may lead to ambiguities. This ambiguity was clarified in [32]. It is far more illuminating to describe the steps in his work than to go through them all: the Fokker-Planck equations for both discretizations were determined, and then, these Fokker-Planck equations were both required to have the thermal equilibrium distribution as a stationary solution. This gave a relationship between the second derivative terms of the Fokker-Planck equation, which made the two discretization schemes equivalent.

The relativistic generalization of these equations is what is used in the remainder of this work; the subscripts L and T were supressed, making the non-relativistic and the relativistic equations look identical without knowing the Gaussian distributions from which the noise terms are drawn. However, the drag term (and consequently, κ) are assumed to be momentum-independent. This is reasonable for the $\bar{c}c$ pairs which actually contribute to the yields of charmonium.

3.3 Langevin dynamics for charmonium

Charmonium can be described, classically, with "Langevin-with-interaction" dynamics:

$$\frac{dp_i}{dt} = -\eta p_i + \xi_i(t), - \frac{\partial U}{\partial x_i}, \tag{3.7}$$

where x_i is simply the coordinate conjugate to p_i and U is the potential energy describing the interaction of two charm quarks. Each element of the ensemble will be a single $\bar{c}c$ pair. The initial distribution of pairs is determined using PYTHIA, an event generator for simulations of particle physics experiments which works at leading order in perturbation theory [33]. The event generator is set for proton-proton collisions at $\sqrt{s} = 200$ GeV, meant to approximate a single nucleon-nucleon collision within a larger heavy-ion collision at the RHIC. Two spatial diffusion coefficients, both relatively small, are considered, as well as a potential energy fitted to lattice results for the internal energy of a color singlet. The temperature is kept at a constant $T = 1.1T_c$, about average for a central gold-gold collision, and the ensemble is evolved.

3.3.1 Evolution of the probability to be bound: The "slowly dissolving lump"

The evolution of the probability for a $\bar{c}c$ pair in this ensemble to be bound is shown in Figure 3.3.1. Discussion of the determination of whether or not a pair in the ensemble is bound can be found in the Appendix, as well as some interesting discussion of Wigner quasi-probability distributions.

In every case plotted, the probability for the pair to be bounded approaches zero. This makes sense: for any single pair in an infinite volume, the expectation value for the separation of the pair increases without bound. Another interesting feature is the small increase in the probabilities at very short times. This is due to the rapid thermalization of the pairs in momentum space; when the diffusion coefficient is relatively small, drag and momentum diffusion coefficient are correspondingly very large, and the distribution in momentum space rapidly changes from being relatively hard to being thermal, leading to an enhancement in the probabilities.

Now, compare the various curves. Clearly, changing the spatial diffusion coefficient has a significant effect. During most of the evolution of the pairs, the ensemble can be characterized as a "slowly dissolving lump", and increasing the spatial diffusion coefficient naturally increases the rate of diffusion. Also important during this stage is the potential energy term. When the ensemble evolves without an attraction between the constituent quarks in the pairs,

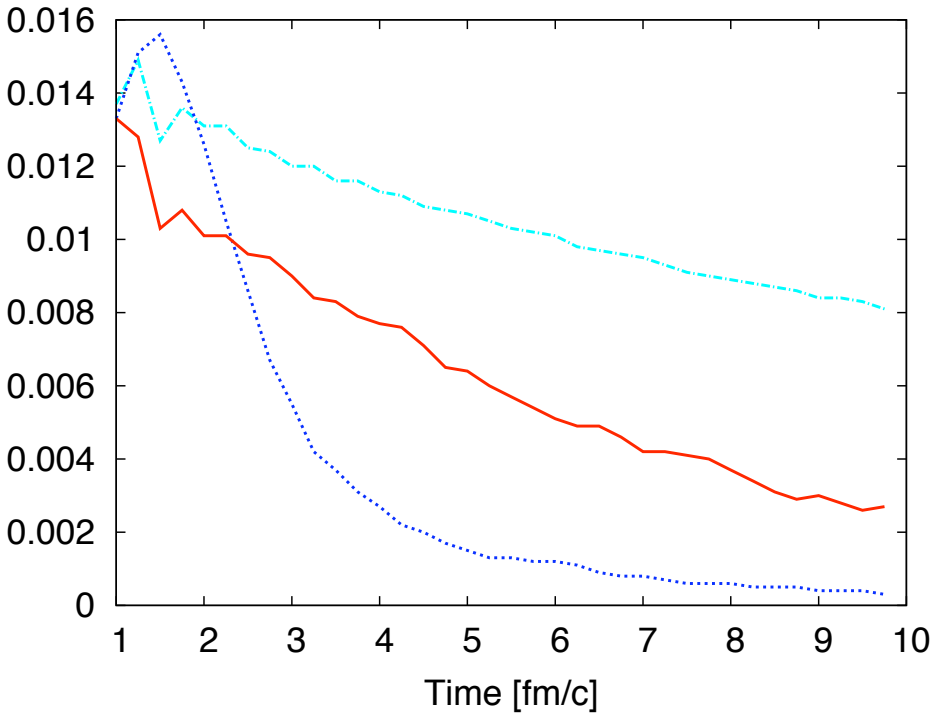

Figure 3.1: (Color online) The probability for a $c\bar{c}$ pair to be bound, where $T = 1.1T_c$ is held fixed. The dotted (blue) curve shows a simulation without a pair interaction and $2\pi TD_c = 1.5$, the solid (red) curve $2\pi TD_c = 1.5$ with pair interaction, and the dot-dashed (green) curve $2\pi TD_c = 3.0$ with interaction.

the rate of diffusion is greatly enhanced. Clearly in this setup, the potential energy of the pair has a significant effect on the final probability for a pair to be bound.

Finally, note simply how D_c, the mass of the charm quark m, and the temperature T set the timescales of this process to be on the order of 1 fm/c, the same order of magnitude of the deconfined phase created in heavy-ion collisions. This suggests a radically different approach for understanding J/ψ suppression: the suppression is due to an *incomplete*, dynamical process and not due only to changes in the spectrum of charmonium above deconfinement.

3.3.2 The density of states: "Quasi-equilibrium"

Figure 3.3.2 shows the formation of "quasi-equilibrium" in the classical ensemble of $\bar{c}c$ pairs undergoing Langevin-with-interaction dynamics [1]. While the true equilibrium of course corresponds to complete dissolution of a single $\bar{c}c$ pair, it turns out that leakage to large distances affects the distributions of separation and energy in normalization only. Figure 3.3.2 shows the energy distribution for the ensemble of pairs at $\tau = 9$ fm/c after evolving under Langevin dynamics at a fixed temperature $1.05T_c$, and it is shown to be the same distribution, up to normalization and statistical uncertainty, as the distribution reached by the pairs in a full heavy-ion simulation of the most central collisions.

The energy distribution in this region is related to a very important issue of exicted charmonium production, namely production of $\psi^{'}, \chi$ states and subsequent feeddown into the J/ψ. When a quasi-equilibrium distribution is reached, the production *ratios* of charmonium states are stabilized at thermal (statistical) model values, in spite of the fact that the overall normalization continues to shrink due to leakage into infinitely large phase space at large distances.

(The energy distribution itself contains a Boltzmann factor but also the density of states. A model case of purely Coulomb interaction allows one to calculate it in a simple way: as shown in the Appendix, the absolute shape of the quasi-equilibrium distribution is reproduced as well.)

The existence of quasi-equilibrium is in good correspondence to observations. It was noticed already a decade ago [34] that in the SPS data on centrality dependence, the $N_{\psi'}/N_{J/\psi}$ ratio approached the equilibrium value

[1] This situation should not be confused with stationary nonequilibrium solutions of the Fokker-Planck equation, in which there is a constant flow through the distribution because of matching source and sink.

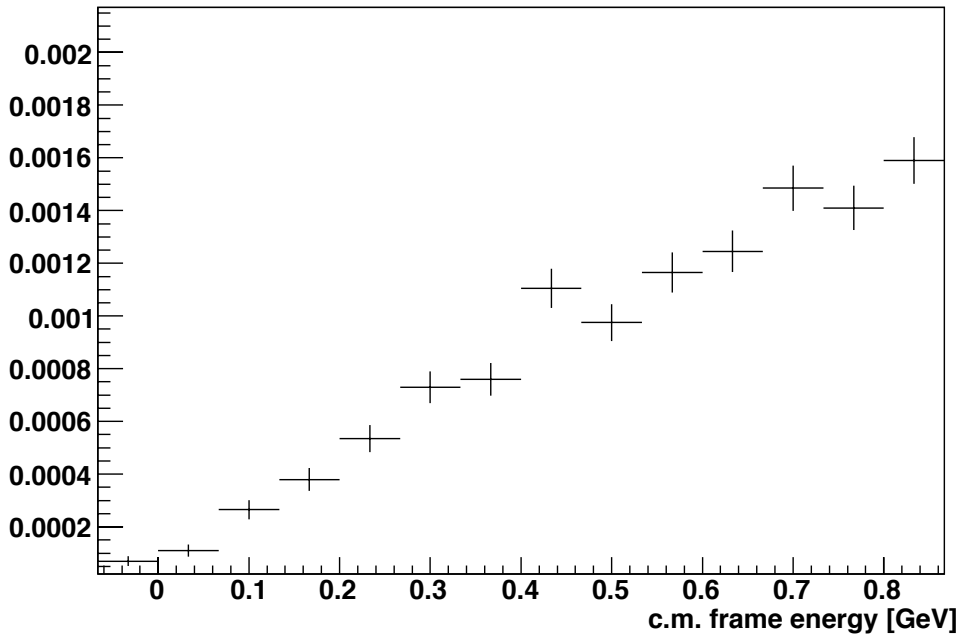

Figure 3.2: Energy distribution of the $c\bar{c}$ pairs (in the center of mass frame of the pair) after Langevin evolution at a fixed temperature $T = 1.05T_c$ for a time $t = 9\ fm/c$ long enough for quasiequilibrium to be reached.

(for chemical freezout)

$$\frac{N_{\psi'}}{N_{J/\psi}} = \exp(-\Delta M/T_{ch}) \tag{3.8}$$

with the chemical freezout at $T_{ch} = 170\,\mathrm{MeV}$, as is observed for ratios of other hadronic species.

One possible explanation of it can be charmonium *recombination* (from independent charm quarks) at chemical freezout, advocated by [35] and others. However the same ratio naturally appears even for a *single* $\bar{c}c$ pair dissolving in a thermal medium. Especially at SPS, when statistical recombination requires a charm density which is too large, this is an attractive possibility.

3.4 Summary

The description of Brownian motion with a Langevin dynamics is of fundamental importance when it comes to describing the dynamics of heavy particles in a sufficiently lighter medium. This description is natural for charm quarks at temperatures just above deconfinement. The Langevin equation includes a stochastic term, making the trajectory of any single particle somewhat unenlightening and requiring functional integrals over the observables in question.

When this description is applied to both of the charm quarks in a charmonium bound state, and temperature and drag are estimated according to what we know about QCD, two important phenomena are present: the evolution of the overall yield of bound charmonium states changes on timescales *of the same order* as those of heavy-ion collisions at the RHIC, and the relative abundances of the various charmonium states quickly approach a state of "quasi-equilibrium", where the relative yields are the same as would be predicted by Boltzmann factors while the overall yield continuously decays. These two properties are in qualitative agreement with the results from PHENIX. The next chapter will discuss a simulation of an ensemble of charm quark pairs that models the gold-gold collisions at the RHIC at various impact parameters, and the results of these simulations will be compared with the PHENIX analysis.

Chapter 4

The Langevin-with-interaction model and charmonium in heavy ion collisions

This model for the dynamics of quarkonium during the hydrodynamical phase should now be applied to gold-gold collisions at the RHIC, and the results compared with observables utilizing the excellent momentum resolution of the PHENIX detector. In Section 4.1, heavy-ion collisions in general are reviewed, with some attention paid to the hydrodynamical description of the quark-gluon plasma phase. The following sections focus on the results of this model, found in [37, 39], with Section 4.2 discussing the initial distribution of charm quark pairs generated, Section 4.3 discussing how these pairs are evolved in a hydrodynamical simulation of the plasma phase, and Section 4.4 how recombinant production should be taken into account.

4.1 Heavy ion collisions: a brief review

4.1.1 The hydrodynamical approach to high-energy collisions

Fermi first suggested using statistical methods in the study of high-energy cosmic ray events [40]. However, Landau's work made the use of hydrodynamics a truly viable option [41]. He noticed several important points: first of all, that in relativistic collisions, it is not the total number of particles produced that is conserved but instead, the macroscopic energy-momentum tensor $T^{\mu\nu}$. In the limit of vanishing mean-free path for the "quasi-particles" of the system, this tensor has a form related to the average flow velocity of a small space-time

volume:

$$T^{\mu\nu} = (e+p)u^\mu u^\nu - pg^{\mu\nu}, \tag{4.1}$$

where p is the pressure and e is the energy density, related to each other through an equation of state. The viscous corrections determined by a small but non-vanishing mean free path, while extremely important in their own right for RHIC phenomenology, are not covered here, for coverage of these terms see [42]. Landau also noticed that, in the absence of shock waves and of large viscous terms, the expansion of the hydrodynamical system in high-energy collisions is nearly adiabatic with the total entropy conserved. In this way, the total entropy scales with the total energy deposited in the collision region: in the earliest estimates, this was assumed to scale with the total energy like $s^{1/4}$ where $s = (P^\mu_{tot})^2$. This proportionality, known as "Landau scaling", seems to predict the total multiplicities in high energy collisions, both in e^+e^- collisions where thermalization surely does not occur and in heavy-ion collisions, where many have argued thermalization does occur.

4.1.2 QCD, heavy-ion collisions, and achieving temperatures above deconfinement

It is interesting to note here how in the history of science, physicists have to be not only clever and creative, but also brave. In 1954 Yang and Mills [43] developed theories with non-Abelian gauge-invariance, where the gauge group is $SU(N)$ and the action is simply the generalization of the field strength squared:

$$\begin{aligned} L &= -\frac{1}{4}F^a_{\mu\nu}F^{\mu\nu a}, \\ [D_\mu, D_\nu] &= -igT^a F^a_{\mu\nu}, \\ D_\mu &= \partial_\mu - igT^a A^a_\mu, \end{aligned}$$

where T^a are simply the generators of the Lie group, defined by these generators' Lie algebra $[T^a, T^b] = if^{abc}T^c$. Written in this way, the geometric simplicity and beauty of their generalization can easily be seen; in the language of fiber bundles, the fibers are now $SU(N)$ instead of $U(1)$, and all the other changes propagate through the usual definitions of connections, covariant derivatives, field strengths, and finally, the action. However, Yang and Mills were trying to describe the strong interaction by promoting isospin to being a local gauge invariance, which is incompatible with what was known even then about the nucleon-nucleon interaction. Yang and Mills had to endure harsh criticism from Pauli and some of the other conservative voices in

physics.

Work on the experimental side of particle physics continued concurrently. For a long time after Landau, particle physicists were more interested in discovering the many new particles than they were with describing collective phenomena in collisions yielding high multiplicities. The quark model made sense of the many mesons and baryons discovered; mesons and baryons are composite particles and members of multiplets that are representations of approximate "flavor" symmetries [44]. This led to the hypothesis that the mesons and baryons must consist of quarks that have spin 1/2 and therefore, if they are to have the proper fermionic statistics, must have an additional degree of freedom. If the quark "color" corresponded to the quarks forming fundamental representations of $SU(3)$ gauge symmetry, antisymmetric statistics could be satisfied.

Around the same time, Yang-Mills gauge theories were found to have a notable quality. The renormalization group equation for $SU(N)$ gauge theory (coupled to N_f flavors of massless fermions that are fundamental representations of the gauge group, simply by replacing ∂_μ with D_μ in the Dirac Lagrangian) has the beta function [45, 46]

$$\beta(g) = \frac{g^4}{16\pi^3}(-\frac{11}{6}N + \frac{1}{3}N_f). \tag{4.2}$$

Integrating this equation gives a coupling constant which depends on mass scale in such a way that at very high energy scales, the coupling constant that represents QCD at all orders best is very small. These gauge theories are therefore asymptotically free, just like the constituent partons in deep inelastic scattering experiments. Lattice simulations also demonstrate that these gauges theories also have the property of confinement, explaining why color dynamics cannot be seen on a macroscopic scale [47]. In this way, strong interactions gained a comprehensive, and simplifying, explanation in terms of quantum field theory.

My advisor Edward Shuryak rediscovered the work of Landau, and used it to describe the dynamics of quark-gluon plasma [11]. He also anticipated the plasma's effects on the observables still considered today: dilepton production, the yields of mesons, and of course, the effects of plasma on quarkonium. Shuryak estimated the effect of "photo-disassociation" of quarkonium states to be small, which has proven to be incorrect; however, he is also the first to have considered J/ψ suppression with a dynamical approach. Shuryak's work helped spark interest in a new experimental program, whose goal is to use high-energy collisions to create a medium that thermalizes at temperatures above deconfinement, so that the non-trivial phase structure of the QCD fields

can be better understood.

4.1.3 Initial conditions: the Glauber model

Despite the ultimate success of quantum field theory in providing a fundamental theory for strong interactions, as well as the robust lattice QCD approach for calculating time-independent correlation functions, there remains a great deal not understood. As noted in Chapter 2, time-dependent correlation functions which depend on soft scales are difficult to determine starting with first principles. Also, large systems – for example the original problem of strong physics, the nucleus – present difficulties. Heavy-ion collisions both are time-dependent and yield large systems. We, like many others before, approximate the evolution of the collision after some initial thermalization time with hydrodynamics; however, what happens before this initial time remains poorly understood.

One approach to the problem is to use the Glauber model to determine an inital entropy distribution in the transverse plane [48]. The major assumption is that the interaction of each nucleon in the "projectile" nucleus A with the nucleons in the "target" nucleus B can be treated as an independent, binary collision (at the RHIC, where both beams are accelerated to the same momentum, "projectile" and "target" are merely labels that aid in the discussion). Typically, to find the entropy density in the transverse plane for a collision determined by an impact parameter b, the entropy density scales with the density of "wounded" nucleons according to some proportionality factor $dS/dNdy$, which also typically scales with the Mandelstam variables like $s^{1/4}$, as in Landau's initial work with "stopped" colliding particles and with the results from gauge/gravity duality [50].

An entirely different approach, correct in the limit of very high energy collisions, is the approximation of the colliding nuclei with a "color glass condensate" [51]. This approach is of course important for probing the "small-x" scale of parton distribution functions, where of course, the density of gluons should not diverge but instead saturate at some momentum scale. In this way, the evolution of the heavy-ion collision, at the earliest times, can be approximated with the classical Yang-Mills equations. In any event, the entropy densities predicted with the color glass condensate approach can be approximated with the Glauber model [49].

4.1.4 The Bjorken solution

Landau's paper on high-multiplicity collisions included a discussion of the hydrodynamics of a very hot "pancake." For ultra-relativistic heavy-ion colli-

sions, Bjorken first explained the best geometry to consider [52]. He noticed two things: first, that in very high-energy collisions, the expansion should be roughly longitudinal Lorentz-boost invariant, and second, that the transverse extent of the collision region can be approximated as very large, with the system nearly isotropic in the transverse direction.

In this setup, there is a natural choice of space-time coordinates: (τ, x_1, x_2, y), where

$$\begin{aligned} \tau &= \sqrt{t^2 - z^2}, \\ y &= \frac{1}{2} \log\left(\frac{t+z}{t-z}\right). \end{aligned} \tag{4.3}$$

In this (1+1)-dimensional, boost-invariant expansion, the 4-velocity in the usual *Minkowski* coordinates, at a given *rapidity* coordinate y, is given by $u^\mu = (\cosh(y), 0, 0, \sinh(y))$. The divergence is determined by $\partial_\mu u^\mu = \frac{\partial}{\partial t}\cosh(y) + \frac{\partial}{\partial z}\sinh(y) = \frac{1}{\tau}$.

Now, for ideal hydrodynamics, the inner product of the conservation law $\partial_\mu T^{\mu\nu} = 0$ with u_ν yields

$$(u^\mu \partial_\mu) e + (p + e)(\partial_\mu) u^\mu = 0. \tag{4.4}$$

The time derivative in the rest frame of the medium $u^\mu \partial_\mu = \frac{\partial}{\partial \tau}$, finally making the hydrodynamical equations of motion into an ordinary differential equation for the Bjorken geometry:

$$\frac{de}{e+p} = -\frac{d\tau}{\tau}. \tag{4.5}$$

Using

$$\frac{ds}{s} = \frac{de}{e+p}, \tag{4.6}$$

and defining the initial condition $s(\tau_0) = s_0$ (where τ_0 is usually, and always in this work, an approximate time for thermalization of the medium), the Bjorken solution describes the scaling of entropy with proper time of fluid elements in the medium:

$$s(\tau) = s_0 \frac{\tau_0}{\tau}. \tag{4.7}$$

For the remainder of this work, the hydrodynamics will be determined with (2+1)-dimensional equations of motion, where longitudinal Lorentz boost invariance is assumed to hold approximately in the geometry of the collision and therefore eliminates the dependence on the rapidity coordinate y. The relativistic equations are solved using finite element methods as in [53]. As

always, I am in a great deal of debt to the work in [38]; the hydrodynamical code is theirs.

4.1.5 The equation of state for QCD at finite temperature

A great deal of work has gone into understanding the equation of state of strongly-interacting matter at finite temperatures and chemical potentials. For finite temperature yet vanishingly small chemical potential, lattice QCD simulations are very well suited for studying the equation of state; it depends only on static quantities that can interchangeably be calculated in real-time or imaginary-time formalisms. The greatest difficulty with the lattice QCD approach is dealing with fermions on the lattice; the latest work with 2+1 flavors of staggered quarks can be found in [54]. The equation of state with fermions has the feature of a "crossover" transition: no discontinuities in any measured derivatives of thermodynamical quantities but a short temperature range, near T_c, where the matter is extremely soft and the entropy density rapidly changes.

This equation of state can be approximated with the equation of state for a system with a "mixed phase":

$$c_s^2 = \begin{cases} c_1^2 & e < e_1 \\ c_2^2 & e_1 < e < e_2 \\ c_3^2 & e_2 < e \end{cases} \tag{4.8}$$

where c_s^2 is the squared speed of sound in the medium. To illustrate the thermodynamical relations needed to simulate hydrodynamics in heavy-ion collisions, we will consider this type of phase transition as in [38].

When the baryonic density is held fixed, manipulating the thermodynamic identities yields the relationship between pressure, energy, and entropy $\frac{ds}{s} = \frac{de}{e+p(e)}$. Also using $\frac{dp}{de} = c_s^2$, the definition of the squared sound speed, entropy density can be determined as a function of energy density:

$$s(e) = \begin{cases} s_0\left(\frac{e}{e_0}\right)^{1/(c_1^2+1)} & e < e_1 \\ s(e_1)\left(\frac{(c_2^2+1)e+(c_1^2-c_2^2)e_1}{(c_1^1+1)e_1}\right)^{1/(c_2^2+1)} & e_1 < e < e_2 \\ s(e_2)\left(\frac{(c_3^2+1)e+(c_2^2-c_3^2)e_2+(c_1^2-c_2^2)e_1}{(c_2^2+1)e_2+(c_1^2-c_2^2)e_1)}\right)^{1/(c_3^2+1)} & e_2 < e \end{cases} \tag{4.9}$$

Finally, the relationship between energy and temperature can be determined using the definition of temperature, $T \equiv \left(\frac{ds}{de}\right)^{-1}$. Knowing the entropy density

at some (usually very high) temperature determines fully the relationships between energy density, pressure, entropy density, and temperature.

In fact, for most of the remainder of this work, the equation of state is assumed simply to be that of an ultrarelativistic gas, where the temperature is the only mass scale of the problem and therefore the proportionalities in the various thermodynamical identities are simply determined by dimensional analysis. This did not change the results significantly yet greatly simplified simulation. The equation of state, using the relations determined above, and the conservation law for the energy-momentum tensor, form a complete set of equations, and the equation of state can be used to determine energy and pressure distributions from any initial entropy distribution in the transverse plane.

4.1.6 Experimental observables and a brief introduction to the RHIC detectors

All heavy-ion physicists, including theorists, need to have some understanding of the capabilities of the detectors at the three major experiments (the SPS, the RHIC, and the LHC). The RHIC, at one time, was the largest machine in the world, and it is definitely inappropriate here to describe the important technical achievements which made possible the acceleration of highly luminous beam of gold nuclei to factors of $\gamma \sim 100$. Here is a brief review of the capabilities of the RHIC detectors, as summarized in Letessier and Rafelski [8]:

The PHOBOS detector focused on examining global properties of heavy-ion collisions. It is a relatively small arrangement of silicon-based detectors that covers a pseudo-rapidity range of $-5.4 < \eta < 5.4$. It has published results on the multiplicity of low-momentum particles. Its results are significant due to its broad rapidity coverage: it demonstrates the flatness of the yield in multiplicity with rapidity and shows how Bjorken's solution can work for describing the hydrodynamics near mid-rapidity.

The BRAHMS detector also covers a large rapidity range ($0 < \eta < 4$) but also a larger transverse momentum range, up to 30 GeV.

The STAR collaboration operates a larger detector consisting of an inner silicon-vertex detector, surrounding the interaction region between 5 and 15 cm, which is also surrounded by a time-of-flight array about 2.5 meters from the the initial interaction vertex. The entire volume has a constant 0.5 T magnetic field, which allows identification of the various charged particles which, combined with the vertex detection, allows excellent measurement of strangeness production. The detector operates with a relatively large rapidity

coverage ($-2 < \eta < 2$) with a low-momentum cutoff of 60 MeV.

Finally, the PHENIX collaboration provides results that inform my work the most, because of both its excellent mass resolution of dielectron pairs in the invariant mass range of charmonium, and because of the detector's relatively rapid data collection, providing very high statistics for the collaboration's results. The two arms of the detector actually cover a small rapidity range ($-0.35 < \eta < 0.35$); also, each arm only covers about $\pi/2$ of the azimuthal range. However, the PHENIX detector combines inner tracking detectors with calorimetry to both leptons, photons, and pions with excellent momentum resolution. The detector is optimized for the measurement of leptons and photons. About 5% of J/ψ particles decay into dielectron pairs and contribute to the yields measured in the PHENIX. An upgrade of the detector will include vertex tracking near the interaction region and allow another measurement important for my work: b-tagging.

To conclude this section: for the study of charmonium, momentum resolution and rapid data acquisition are more important than broad rapidity coverage, making PHENIX the detector most important for my work. Vertex detection at the PHENIX make the study of bottom, bottomonium, and $b\bar{c}$ states an exciting possibility for future runs.

4.2 Production of the initial $\bar{c}c$ pairs

Here begins a detailed description of my work in using Langevin-with-interaction simulations, where flow and temperature are determined with a (2+1)-dimensional "Bjorken-like" hydrodynamical simulation, to determine changes in the yields of charmonium states during the plasma phase. It begins with determining an initial distribution for the ensemble. This first step is unfortunately also the hardest, since there is not way to measure experimentally these initial distributions in a heavy-ion collision and there are many changes expected from proton-proton collisions to nuclear collisions due to "cold-nuclear matter" effects, for example, shadowing and anti-shadowing of the parton distribution functions [55], absorption and breakup of charmonium due to the many nucleons present [56], and possibly also the gluon saturation that affects heavy-ion collisions [57] [1]. We will not go into the details of any of this here: we simply use leading-order event generation as something of a "place-holder", and model the effect of the plasma phase on yields and determine the relative change.

[1] While Tuchin's work concerning the effects of gluon saturation makes clearly important points, I cannot agree that it explains all J/ψ suppression; his only source of charmonium is the yield of states with quantum numbers identical to the corresponding final states, which cannot explain the overall yields even in proton-proton collisions.

The initial distribution of $\bar{c}c$ pairs are generated with PYTHIA, a particle physics event generator [33]. PYTHIA yields $\bar{c}c$ pairs through a set of perturbative QCD events: through Monte-Carlo it will selectinitial partons from the parton distribution function of one's choosing and proceed through leading-order QCD differential cross sections to a random final state.

By using PYTHIA we do not however imply that it solved many open issues related with charmonium production, such as color octet versus singlet state. It also leaves open the very important issue of $feeddown$ from charmonium excited states, as will be seen in Section 4.3.2. One more open question – needed to start our simulations – is how to sample the distribution in position space. Indeed, each pQCD event generated in PYTHIA is a momentum eigenstate without any width, so by Heisenberg's uncertainty relation they are spatially delocalized, which is unrealistic.

We proceed assuming the form for the initial phase-space distribution to be

$$P_{\rm init}(\mathbf{x},\mathbf{p}) \propto P_{\rm PYTH}(\mathbf{p}) \exp(-\mathbf{x}^2/2\sigma^2) \tag{4.10}$$

By setting $\sigma = 0.3$ fm one can tune the energy distribution to give a reasonable probability for the formation of J/ψ state in proton-proton events.

However this does *not* yield correct formation probabilities of χ, ψ'. It is hardly surprising, since for example the ψ' wavefunction has a sign change at certain distances, so because the exact production amplitude is required for a projection, an order-of-magnitude size estimate is not good enough. Since feeddown from those states contributes about 40% of the observed J/ψ, we simply refrain from any quantitative statements about proton-proton (and very peripheral AA) collisions, focusing only on distributions $after$ some amount of time spent in QGP, which is when simply statistical hadronization has some predictive power [58].

4.3 Langevin motion of $\bar{c}c$ pair in an expanding fireball

The motion of a charm quark pairs is simulated in a hydrodynamical simulation of the quark-gluon plasma phase of gold-gold collisions [38]. The same framework and programs used in [19] used to examine motion of a single charm quark has been used for the simulation of an interacting pair.

We start with large number of $\bar{c}c$ produced with PYTHIA pQCD event generation, and randomly place them in position space throughout the fireball, using a Monte-Carlo Glauber calculation.

Then, the pairs are evolved in time according to the Langevin equation

with a force term:

$$\frac{d\mathbf{p}}{dt} = -\eta\mathbf{p} + \xi - \nabla U, \tag{4.11}$$

$$\frac{d\mathbf{x}}{dt} = \frac{\mathbf{p}}{m_c}. \tag{4.12}$$

where ξ is a random force and η the drag coefficient. We proceed here with our diffusion constant set to be $\eta_D = \frac{2\pi T^2}{1.5M}$ and half of this value, which are large values relative to other works, in the spirit of Chapter 2.

Now we examine the evolution of the quark pairs as discussed before, examining pairs at mid-rapidity in a boost-invariant, 2-dimensional ultra-relativistic gas simulation, the same hydrodynamical simulation used in [19]. We stop the Langevin-with-interaction evolution when $T < T_c$. The distribution over energy at different moments of the time is shown in Fig.4.3.

4.3.1 Shadowing and "normal" absorption

Experimental data include not only the "QGP suppression" we study in this work, but also (i) the initial-state effects (modified parton distributions in "cold nuclear matter") plus (ii) the so called "normal nuclear absorption." For a long time, all of these effects were parametrized with a single parameter, a "disassociation cross section" [64]:

$$R_{pA} = exp(-\sigma_{abs}\langle L\rangle n_0), \tag{4.13}$$

where $\langle L\rangle$ is the mean path length of the J/ψ through nuclear matter, n_0 is the nuclear density, and $\sigma_{\rm abs}$ is the nuclear absorption cross-section (parametrized from [64] to be 0.1fm^2 for rapidity $y = 0$). For rapidity $y = 0$, this can be rewritten as $(R_{pA}(y = 0))^2 = \exp(-\sigma_{abs}\langle N_{part}\rangle$, where $\langle N_{part}\rangle$ is the density per unit area of participants in the collision plane. Glauber model calculations [65] determine $\langle N_{part}\rangle$ for a given $N_{\rm part}$ at PHENIX. Each Au+Au data point from PHENIX is divided by this quantity and called $R_{AA}^{anomalous}(y = 0)$, plotted in Figure 4.3.2.

4.3.2 ψ' production and feeddown

The ratio $N_{\psi'}/N_{J/\psi}$ is calculated in the simulations, for different centralities. There are well known NA38/50/60 measurements of this ratio at the SPS, but at RHIC it has been measured so far only in proton-proton collisions by the PHENIX detector [68] to be 0.14 ± 0.04, which makes the ratio of direct ψ' to J/ψ particles 0.24 as in [67]. Hopefully higher luminosity at RHIC will make

possible a future measurement of this ratio in Au+Au collisions of various centralities.

$N_{\psi'}/N_{J/\psi}$ is determined as follows: (i) first we run our simulation and determine the distributions $f(E)$ over the $\bar{c}c$ pair energy $E = E_{CM} - 2M_c$ (in the pair center of mass frame); (ii) these are compared with the quasi-equilibrium distributions from simulations at fixed temperature (slightly above T_c) $f_0(E)$. This complicated procedure is the result of the simple fact that all along, we have never claimed to be able to determine well the initial yields of the various charmonium states; we have no interest in making claims in this area, and we simply wish to determine changes in these yields due to dynamics during the deconfined phase, of which we do claim to have some understanding. This is possible for us simply due to the fact that in $f(E)/f_0(E)$, the density of states is divided out. This ratio determines how different the actual distribution is from that in quasi-equilibrium. Next (iii), the *double* ratios are determined, at two relative energies corresponding to $\psi^{'}$ and J/ψ masses (minus $2m_{charm}$)

$$R_{\psi'/J\psi} = \frac{f(.8\text{ GeV})}{f_0(.8\text{ GeV})} / \frac{f(.3\text{ GeV})}{f_0(.3\text{ GeV})}. \tag{4.14}$$

This now includes nonequilibrium effects. Finally (iv), the particle ratio is a combination of nonequilibrium and equilibrium factors

$$\frac{N_{\psi'}}{N_{J/\psi}} = R_{\psi'/\psi} \exp(-\Delta m/T) \tag{4.15}$$

The double ratio (or $\exp(\Delta M/T) N_{\psi'}/N_{J/\psi}$) is plotted versus centrality in Fig. 4.3.2, for two values of the diffusion coefficient.

As one can see, it goes to unity for the most central collisions: so quasi-equilibrium is actually reached in this case. One can also see that this quasi-equilibrium is reached quicker for a smaller diffusion coefficient, as it should. For mid-central bins the $\psi^{'}$ production is about twice larger because of insufficient time for thermalization. This is to be compared to the experimental proton-proton value for the ratio, which is about 5.

Finally, this result should be used to estimate the effect of feeddown from higher states. The final number of J/ψ particles observed is the number of directly produced J/ψ particles plus the number of J/ψ particles produced from feeddown from higher charmonium states:

$$N_{J/\psi}^{final} = N_{J/\psi}^{direct} \left[1 + R_{\psi'/\psi} \sum_i (\frac{g_i}{3}) \exp(-\frac{\Delta M_i}{T}) B_i \right] \tag{4.16}$$

where i is summed over the χ_1, χ_2, and ψ' particles which contribute significantly to feeddown, B_i represents their branching ratio into $J/\psi + ...$, and g_i is the degeneracy of the state (divided by 3, the degeneracy of the J/ψ), Δm_i is the mass difference between the i-th state and the J/ψ. The $R_{\psi'/\psi}$ is the non-equilibrium factor discussed above: it is factored outside the sum because it is very similar for all these states.

Now consider centrality dependence of the J/ψ production *including* the feeddown. Define for each centrality direct $N_{J/\psi}^{direct}(b)$ as the total number of $c\bar{c}$ pairs in our ensemble with energy (in its rest frame) less than $E < 2M_{charm} + 0.33$ GeV. Feedown gets its dependence on centrality from $R_{\psi'/\psi}(b)$ determined from simulation.

Finally, R_{AA} as a function of the number of participants is determined by normalizing the final yields of J/ψ with initial yield from PYTHIA (with feeddown included) for a very peripheral collision, shown in Figure 4.3.2 for various parameters for the Langevin dynamics. Also shown, for the case of $2\pi T D_c = 1.5$ with the potential on, are various levels of sophistication for determining R_{AA} in the same simulation: one where we simply assume $R_{AA} = S_{bound}$, one where R_{AA} is determined with only direct J/ψ states, and one where proper feeddown probabilities are included. Although the results are less dramatic than what Figure 3.3.1 would suggest, we plainly see that the predictions of our model are sensitive to the value of the diffusion coefficient, and a small diffusion coefficient with the charm and anti-charm quarks in a pair interacting can help explain why the suppression observed at the RHIC is on the order of the suppression observed at SPS.

4.3.3 Including the "mixed phase"

So far, only the evolution of the $c\bar{c}$ pairs during the QGP phase has been simulated, stopping the evolution wherever the fluid's temperature reached T_c. The heavy-ion collisions at RHIC seem to proceed through a "mixed phase" for central and semi-central collisions, where the medium spends a significant amount of time near T_c, as described in [38]. For our determination of R_{AA} versus N_{part}, the mixed phase is insignificant: the percentage of J/ψ particles does not change significantly after the initial as Figure 3.3.1 suggests. Since we do not pretend to know the dynamics of charmonium in the mixed phase, we are satisfied that even the extreme limit of unchanged Langevin evolution through the mixed phase does not significantly change our results in Figure 4.3.2. However, for describing the development of momentum anisotropy of charmonium in a semi-central collision ($v_2(p_t)$), the mixed phase is of great importance and we are forced to model it for a typical collision in the minimum

bias data set.

In various hydrodynamic models which describe heavy ion collisions, the region of roughly $T = 0.9 - 1.1\ T_c$ is treated as a separate "mixed phase" distinct from QGP and hadronic phases. Indeed, it has a very different equation of state: while the temperature and pressure remain nearly constant, the energy and entropy densities jump by a large factor [2].

What is very important for the present paper is that the near-T_c region occupies a significant fraction of the hydrodynamical evolution, in spite of being a very narrow interval in terms of T. Indeed, one should rather focus not on T but on the entropy density s, which shows a simple monotonous decrease with time $s \sim 1/\tau$ for all three phases.

For a quantitative description of the mixed phase we used hydrodynamical calculations, known to describe radial and elliptic flow well, such as the work by Shuryak and Teaney [38]. It follows from their solution that the "mixed phase" persists for about $5\,\mathrm{fm}/c$ after the deconfined phase, which is comparable to the lifetime of the deconfined phase at the very center of the transverse plane. Thus it is by no means a small effect, and should be included in any realistic treatment of a heavy-ion collision.

The flow during this time was found to be well approximated by Hubble-like expansion with radial velocity $v = Hr$ and time-independent $H \approx 0.075\,\mathrm{fm}^{-1}$ for central collisions. For a collision with a nonzero impact parameter (below we will consider $b = 6.5\,\mathrm{fm}$), the anisotropy of this expansion can be parameterized similarly:

$$v_i = H_i x_i, \tag{4.17}$$

with $i = 1, 2$ and $H_x = 0.078\,\mathrm{fm}^{-1}, H_y = 0.058\,\mathrm{fm}^{-1}$: thus anisotropy is only about 80% by this late stage. It is fair to say that we have a fairly reasonable understanding of how the medium flows for these later stages: thus in our simulations we have used those parameterizations instead of numerical solutions to hydrodynamics, which were necessary for the QGP phase.

Let us start with two extreme scenarios for the dynamics of the charm quarks during this phase of the collision:
1.) the charm quarks are completely "stopped" in the medium, so that they experience the same Hubble-like flow as matter;

[2] Although the exact nature of matter in the near-T_c region is not yet understood, let us mention that the original "mixed phase" description, originating from the notion of the first-order phase transition, cannot be true, as "supercooling" and bubble formation expected in this case are not observed experimentally. Lattice gauge theory suggests a smooth crossover-type transition, with a high but finite peak in the specific heat. Recently there has been renewed interest in this region, after the so-called "magnetic scenario" for it has been proposed [69, 70], describing it as a plasma containing a significant fraction of magnetic monopoles.

2.) $\bar{c}c$ pairs do not interact at all with the medium near-T_c, moving ballistically with constant velocity for the corresponding time in the collision.

If the first scenario were true, the effect of Hubble flow would be to increase all momenta of particles by the same multiplicative factors $p_i(t) = p_i(0)\exp(H_i t)$. With sufficiently high drag, Langevin dynamics would bring the charm quarks rapidly to a thermal distribution, and since $M >> T$ it is a good approximation in this case to say that the heavy quarks have been "stopped". However, we will show below that at the "realistic" value used for the drag η_c this does *not* happen during the time allocated to the mixed phase, there is instead ongoing "stopping" of the charm quarks relative to fluid elements. (This also will be important for the evolution of the azimuthal anisotropy $v_2(p_t)$ for single charm and for charmonium). The second scenario predicts $v_2(p_t)$ for single charm quarks which is far smaller than what is measured. We do not consider this scenario further even though something might be said for modelling charmonium in the mixed phase as interacting far less than single charm.

Several single charm p_t-distributions are shown in Figure 4.5 (normalized for simplicity to unity). The initial distribution after hard production predicted by PYTHIA is the largest at high p_t: this is compared to the Langevin evolution before (squares) and after (triangles) the mixed phase, for a semi-central RHIC collision ($b = 7$ fm). In order to see that radial flow still is important, we have also shown what happens if Langevin evolution takes place in an unmoving fixed-T plasma (circles).

This comparison demonstrates once again the main point on which the Langevin-with-interaction model for charmonium is based: for charm quarks and charmonium in a heavy-ion collision equilibration is never complete,even in momentum space, making the specific timescales of different phases of matter of fundamental importance.

Unfortunately, in the near-T_c region it is much less clear how to describe the $c-\bar{c}$ interaction. As we have learned from lattice data, the difference between free-energy and potential-energy potentials are very drastic in this case: in the former case the tension (the force from the linear potential) disappears while in the latter it becomes about 5 times stronger than it is in vacuum. As discussed in refs[71, 72], the latter is presumably due to a metastable electric flux tube.

Which potential to use depends on timescales of the $c-\bar{c}$ dynamics, which are not well understood at this point. Therefore we took for now a conservative approach, assuming that at the near-T_c stage charm pairs interact according to the simple Coulomb interaction $V = -\alpha_s/r$. Additionally, in our model for this phase we assume the interaction of the charm quarks with the medium

can be modelled with the same Langevin dynamics with the temperature approximated as a fixed $T = T_c$ and the flow given as above. We found that with the simple Coulomb potential used in the mixed phase, the survival probability dropped slightly but not significantly: and although we do not discuss other possibilities in this work further, in principle this can be changed if the potential to be used has significant tension.

One final interesting observable would be a measurement of charmonium elliptic flow, characterized by the azimuthal anisotropy parameter $v_2 = \langle cos(2\phi) \rangle$, induced by ellipticity of the flow on charm quarks. A measurement with low statistics has been already made at PHENIX [73]: both PHENIX and STAR are working on higher statistics data previously recorded. The result of our calculation of $v_2(p_t)$, both for single charm quarks and for the J/ψ, is shown in Figure 4.6.

Greco, Ko, and Rapp also made predictions for the v_2 for J/ψ [74], with a model where all of the final J/ψ-states coalesced from the single charm quark "thermal+flow" distribution one would get from a typical minimum bias RHIC collision. We have in common strong interaction of charm with the medium, and coalescence from these charm quarks of the observed J/ψ particles. As it turns out, our predictions are similar: v_2 of J/ψ should be less than the v_2 of single charm for low p_t, but then increase past the v_2 of single charm at $p_t > 3$ GeV.

4.4 Recombinant production of charmonium in gold-gold collisions

In the previous section, a possibly important source of charmonium at RHIC was not considered: the "recombinant" contribution of J/ψ particles whose constituent quarks originate from different hard processes. At very high collision energies, as the number of charm pairs per event grows, recombinant charmonia could potentially lead to an enhancement of the final J/ψ yields in a heavy-ion collision, reversing the current suppression trend. Using the grand canonical ensemble approach, Braun-Munzinger and collaborators [58] determine the fugacity of charm by the number of $\bar{c}c$ pairs produced initially. The "statistical hadronization" approach to charmonium assumes complete thermal equilibration of charmonium. Greco, Ko, and Rapp [74] studied how coalescence models, when applied to the single charm momentum distributions predicted both by perturbative QCD and by thermodynamics and flow at the RHIC, can be used to examine this possible recombinant yield. A somewhat different approach has been taken by Grandchamp and Rapp [75], who treat

the J/ψ yields from heavy-ion collisions as coming from two sources: the direct component, which decays exponentially with some lifetime τ_d, and the coalescent component, which is determined by the same mechanism in [58], with the additional consideration that spatial equilibration of charm does not happen. To account for enhanced local charm density, by small spatial diffusion, they had introduced another factor - the "correlation volume" V_{corr} - which was estimated. The present work can be viewed as a quantitative dynamical calculation of this parameter.

To gain insight, let us compare these models with our model in [37]. The Langevin-with-interaction model for $\bar{c}c$ pairs in medium makes no assumptions about complete thermalization, and shows how even in central Au+Au collisions at the RHIC, the majority of the J/ψ yields may survive the QGP phase. However, the model predicts rapid thermalization in the momentum distributions of charmonium, as well as equilibration in the relative yields of the various charmonium states due to the formation of "quasi-equilibrium" in phase space. This requires no fine-tuning of the rates for charmonium in plasma; it is just a natural consequence of the strongly coupled nature of the media, detailed by the Langevin dynamics. However, recombinant production of charmonium may still be an important effect in our model, due to the fact that in central collisions, the densities of unbound charm quarks can be quite high in some regions of the transverse plane.

4.4.1 Recombination in Langevin-with-interaction simulations

As before, we start with a large ensemble of $\bar{c}c$ pairs whose momenta are determined with PYTHIA event generation [33]. The positions of the initial hard collisions in the transverse plane at mid-rapidity are determined by sampling the distribution in N_{coll} determined from the Glauber model. In this way, our local densities of $\bar{c}c$ pairs vary as one would expect from the Glauber model, which gives an enhancement for recombination towards the center of the transverse plane. Each element of the ensemble now contains N $\bar{c}c$ pairs. The number of pairs N depends on the impact parameter of the collision and needs to be determined.

The average number of $\bar{c}c$ pairs for a Au+Au collision at RHIC varies with impact parameter and has been investigated by the PHENIX collaboration at mid-rapidity [76]. The measured cross sections for charm production vary somewhat with the centrality of the collision and achieves a maximum of about 800 μb for semi-central collisions. The nuclear overlap function $T_{AA}(b)$ can be calculated with the Glauber model. We used a convenient program by Dariusz

Miskowiec [77] to evaluate this function. With a centrality dependent cross-section $\sigma_{\bar{c}c}$, we can easily calculate the average number of $\bar{c}c$ pairs in a collision: $N_{\bar{c}c} = T_{AA}\sigma_{\bar{c}c}$. The number of $\bar{c}c$ pairs reaches a maximum in central collisions, with an average of 19 pairs per collision.

In order to determine the probability for two charm quarks from different hard processes to form recombinant charmonium, we must average over the different possible pairings of all of the unbound quarks in each element of our ensemble. This is discussed in the Appendix in generality. Since the number of $\bar{c}c$ pairs approaches 20 for central Au+Au collisions at RHIC, we are faced with another issue: there are 20! possible pairings and it has become impractical to calculate the probability of each individual pairing this way. In general, we would be forced to perform *permutation sampling* of this partition function, preferably with some Metropolis algorithm. How to sample over permutations with a Metropolis algorithm is discussed thoroughly in the literature, for an excellent review of this see Ceperley [90]. However, for RHIC, the situation simplifies due to the relatively low densities of $\bar{c}c$ pairs involved. We ran our simulation for the most central Au+Au collisions at RHIC and examined how many "neighbors" each charm quark had. A "neighbor" is defined as a charm anti-quark, originating from a different pQCD event yielding the given charm quark, which is close enough to the charm quark that it could potentially form a bound state, in other words r is such that $V_{Cornell}(r) < 0.88$ GeV. The number of charm quarks expected to have one and only one neighbor in the most central Au+Au collisions was found to be 5.5%, while only 0.2% of the charm quarks are expected to have more than one neighbor. Therefore, even at the most central collisions at RHIC, we can be spared possibly complicated permutation samplings. Of course, this situation is not true in general, and for the numbers of pairs produced in a typical heavy-ion collision at the LHC one should modify these combinatorics.

4.4.2 Analysis of the data including improved dAu sample

The data with which we now compare our results is different from that which we used for comparison in our previous work. New data analysis of Au+Au and d+Au described in [78] account for the (anti-)shadowing and the breakup of charmonium due to the cold nuclear matter effects (parameterized by σ_{abs}) in the framework of a Glauber model for the collision. The calculations at forward and mid-rapidity are now done independently, since shadowing and breakup could be considerably different at different rapidities. This new analysis is a significant success, demonstrating the high suppression at forward rapidity

(previously very puzzling) as being due to cold nuclear matter effects. New ratios of observed suppression due to cold nuclear matter R_{AA}/R_{AA}^{CNM}, plotted versus the energy density times time $\epsilon\tau$, show common trends for RHIC and SPS data, which was not the case previously. We use this new analysis as a measure of survival probability in our calculation.

4.4.3 The results

Before we show the results, let us remind the reader that our calculation is intended to be a dynamical one, with no free parameters. We use a hydrodynamical simulation developed in [38] which is known to describe accurately the radial and elliptic collective flows observed in heavy-ion collisions. Our drag and random force terms for the Langevin dynamics has one input – the diffusion coefficient for charm – constrained by two independent measurements (p_T distributions and $v_2(p_T)$ measurements for single lepton – charm – performed in Ref. [19]. The interaction of these charm quarks are determined by the correlators for two Polyakov lines in lQCD [63].

Having said that, we still are aware of certain uncertainties in all the input parameters, which affect the results. In order to show by how much the results change if we vary some of them, we have used the uncertainty in the value for the critical temperature T_c. For these reasons, we show the results for two values $T_c = 165,\ 190$ MeV, in Fig.4.7.

As can be seen, a higher T_c value improves the agreement of our simulation with the latest analysis of the data, because in this case the QGP phase is shorter in duration and the survival probablity is larger. However the recombinant contribution (shown by filled squares) is in this case relatively smaller, making less than 1/3 of the yield even in the most central collisions at RHIC.

Zhao and Rapp used the "two-component model" for J/ψ production at the RHIC and also achieved some agreement with the anomalous nuclear modification of J/ψ yields[79]. We would like to point out that the two components in their model ("surviving" and "regenerative" production) are not exactly the same as the two components plotted here ("diagonal" and "non-diagonal"). This by itself is not a criticism of either calculation: it is simply a difference in how the total yield has been separated into two components and modeled, in these two different calculations.

4.4.4 Recombinant J/ψ and p_t-distributions

So far, we have only considered the effect of the recombinant production on the overall yields of J/ψ particles at the RHIC. We should test our model by

considering whether or not adding the recombinant contribution can change the shape of any differential J/ψ yields.

One differential yield where we may expect the surviving and recombinant component to have different behaviors is in the p_T-distributions for central Au+Au collisions. The surviving J/ψ states tend to originate in the periphery of the collision region, since the J/ψ states produced here endure the sQGP phase for the shortest times. However, the recombinant contribution should form toward the center of the collision region, since this is where the density of initial $\bar{c}c$ pairs is highest, and as we have been showing for some time, spatial diffusion is incomplete in the sQGP. Therefore, since the effect due to flow on the p_T-distributions has Hubble-like behavior, with the radial velocity of the medium scaling with distance from the center of the transverse plane, we would expect the recombinant contribution to exist, on average, in regions of the medium with significantly smaller flow velocities.

Figure 4.8 demonstrates this behavior existing in our simulation.

We should now determine whether or not this difference of the yield versus r can be observed in the J/ψ yield versus p_t. As we have shown in our previous paper, during the phase transition from QGP to the hadronic phase in heavy-ion collisions, our model predicts a small change in the total J/ψ yield but relatively large changes in the J/ψ p_t distributions, with these changes strongly dependent on the drag coefficient for quarkonium during this time, and T_c. We can easily run our code with the lattice equation of state, which properly describes the hydrodynamics during this important "mixed phase", and make different predictions for the two components' p_t distributions, depending on various choices for the drag coefficient appropriate in this phase. However, for reasons which will become apparent, we are only interested in the upper limit of the effect of flow on p_t in Au+Au collisions at the RHIC. Therefore, we ran our simulation where we assumed a phase transition which lasts 5 fm/c, during which the J/ψ particles equilibrate rapidly with the medium (in other words, have a relaxation time of zero and mean free path of zero), in a Hubble-like expansion.

The p_t distributions after this expansion are shown in Figure 4.9. It is visible from this plot that the recombinant contribution will observably increase the total yield at low p_t (where the total yield is significantly higher than the surviving component alone) and have little effect at higher p_t (where the total and the surviving component alone are nearly the same). However, we have found that even in this extreme limit, there is no clear signal in the differential p_t yields for there being two components for J/ψ production at the RHIC.

This test, however, should not be abandoned for measurements of the differential yields at higher collision energies. Since the recombinant contribu-

tion grows substantially as charm densities are increased, it should be checked whether or not the recombinant contribution is more strongly peaked in the center of the transverse plane of LHC collisions, and whether or not two components to the differential yields should become observable there. We will follow up on this issue in a work we have in progress.

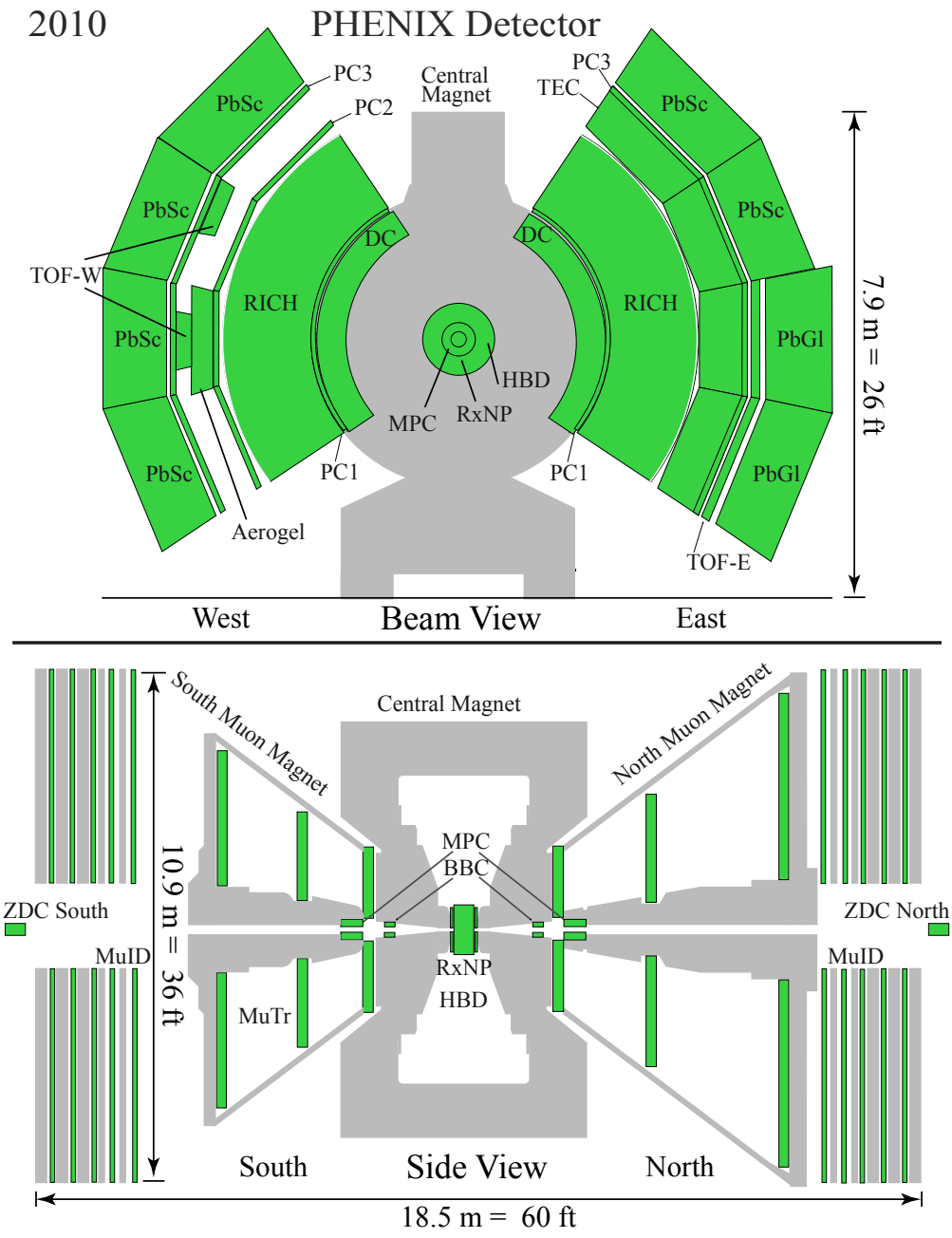

Figure 4.1: (Color online.) A diagram of the PHENIX detector, showing: the zero-degree calorimeters (ZDC), the beam-beam counters (BBC), the drift chambers (DC), the ring-imaging Cherenkov detectors (RICH), and at the ends of the arms, the calorimeters. Courtesy of the PHENIX collaboration.

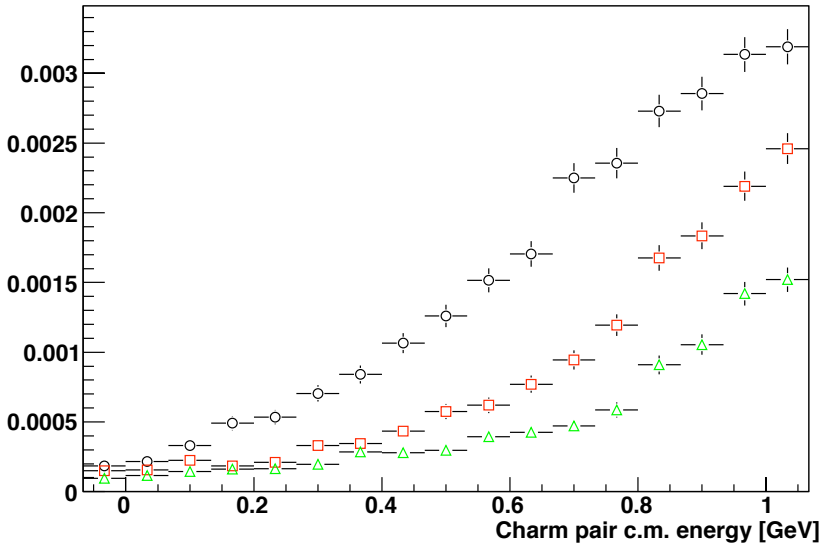

Figure 4.2: (Color online.) Evolving energy distribution for an ensemble of $\bar{c}c$ pairs at time moments $t = 2, 3, 10$ fm/c (circles,squares and triangles, respectively).

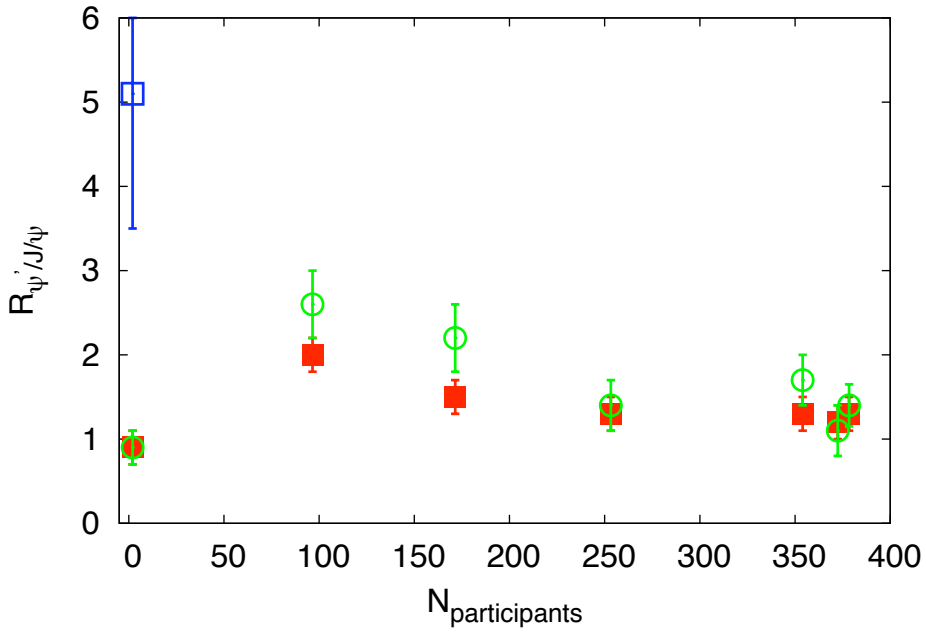

Figure 4.3: (Color online) The ratio $\exp(\Delta m/T_c)N_{\psi'}/N_{J/\psi}$, the open box (blue) represents the measured ratio in pp collisions at the RHIC, the open circles (green) represent the results of our simulation for different N_{part} with $2\pi TD_c = 3.0$, and the solid boxes (red) represent the results of our simulation with $2\pi TD_c = 1.5$.

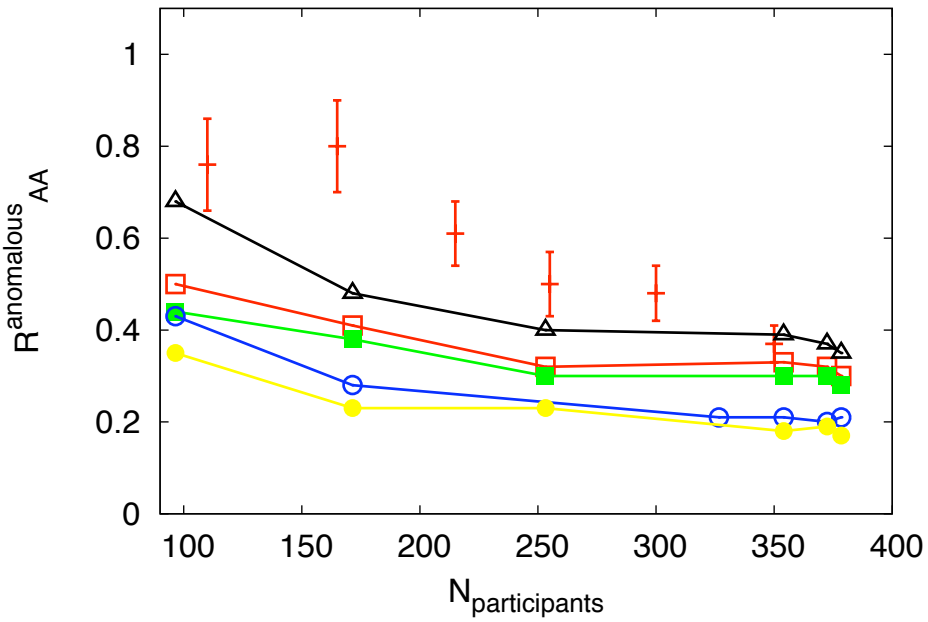

Figure 4.4: (Color online) The RHIC data for R_{AA} vs. N_part for J/ψ (with nuclear effects "factored out") with the results of our simulation. From top to bottom: the open triangles (black) represent S_{bound} for $2\pi TD_c = 1.5$ and the potential on, the open boxes (red) represent R_{AA} for just the J/ψ with feeddown in the same simulations, the solid boxes (green) represent R_{AA} for just the J/ψ without feeddown, the open circles (blue) represent R_{AA} with $2\pi TD_c = 1.5$ and the potential off, and the solid circles (yellow) represent R_{AA} with $2\pi TD_c = 3.0$ and the potential on.

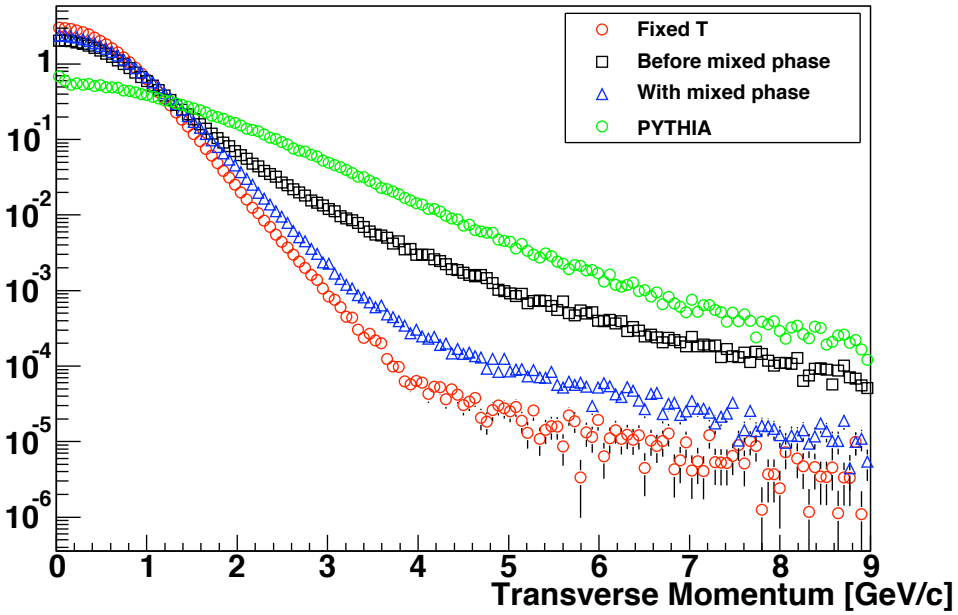

Figure 4.5: (Color online.) The charm p_t-distribution after the mixed phase compared with the distribution without flow, the distribution originating from PYTHIA, and the distribution before the mixed phase

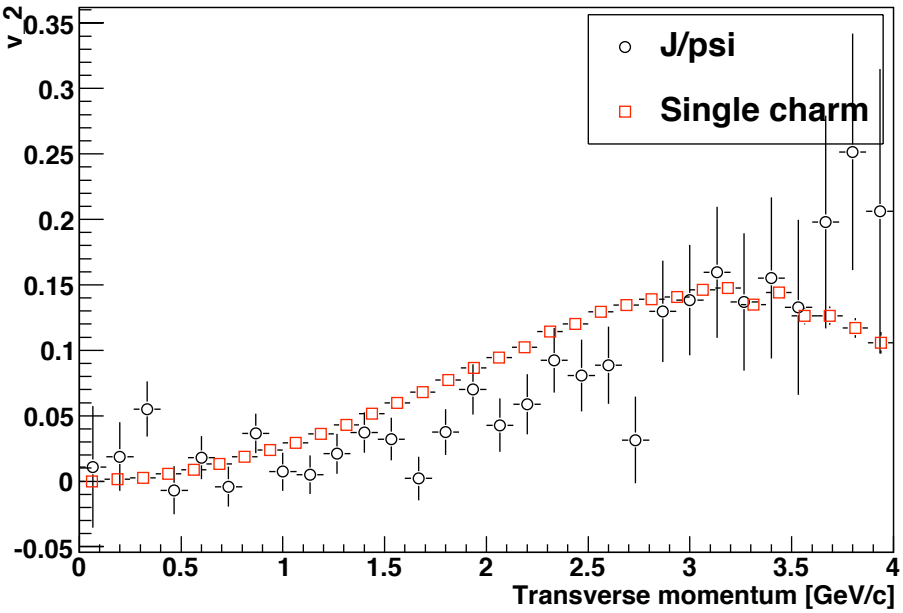

Figure 4.6: (Color online.) The azimuthal anisotropy versus transverse momentum for both single charm and for J/ψ.

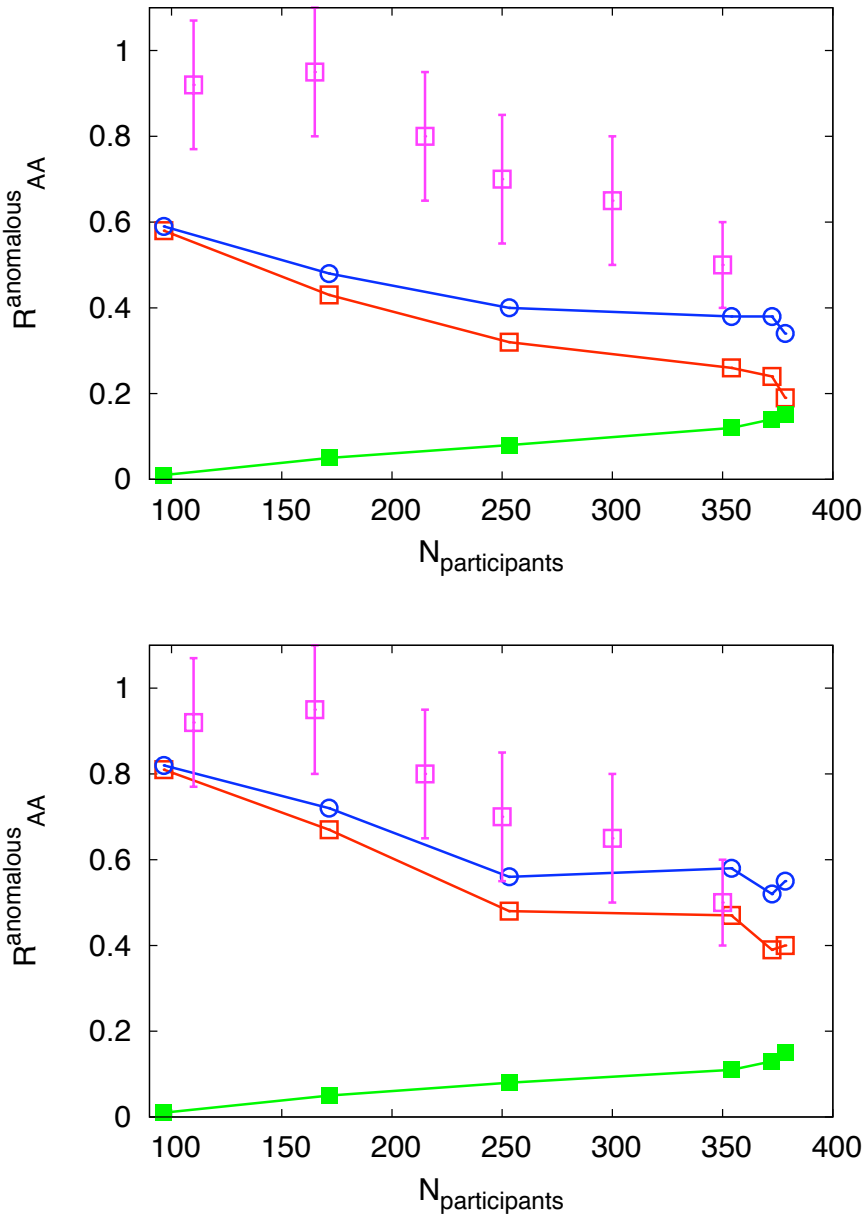

Figure 4.7: (Color online.) $R_{AA}^{anomalous} = R_{AA}/R_{AA}^{CNM}$ for J/ψ versus centrality of the AuAu collisions at RHIC. The data points with error bars show the PHENIX Au+Au measurements with cold nuclear matter effects factored out as in [78]. Other points, connected by lines, are our calculations for the two values of the QCD phase transition temperature $T_c = 165$ MeV (upper) and $T_c = 190$ MeV (lower). From bottom to top: the (green) filled squares show our new results, the recombinant J/ψ , the open (red) squares show the R_{AA} for surviving diagonal J/ψ , the open (blue) circles show the total.

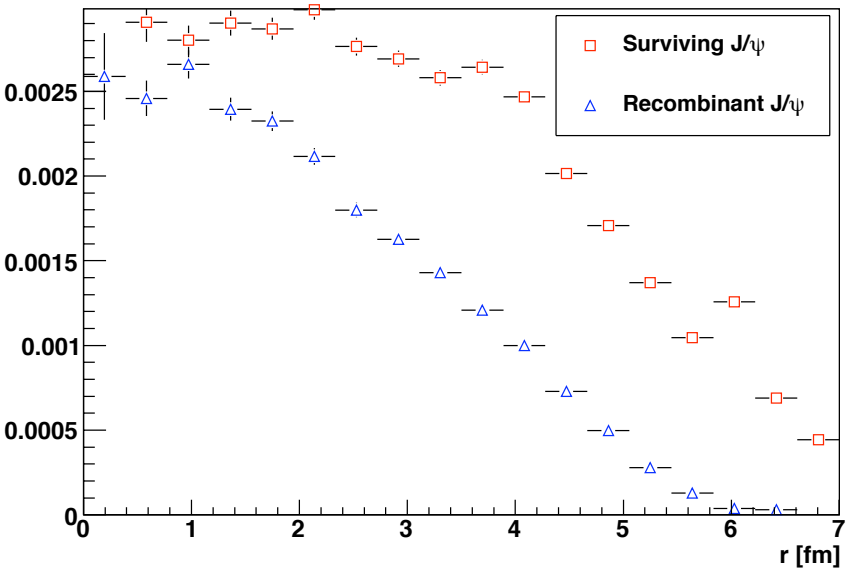

Figure 4.8: (Color online.) The surviving and recombinant J/ψ yields, plotted versus the radial distance from the center of the transverse plane.

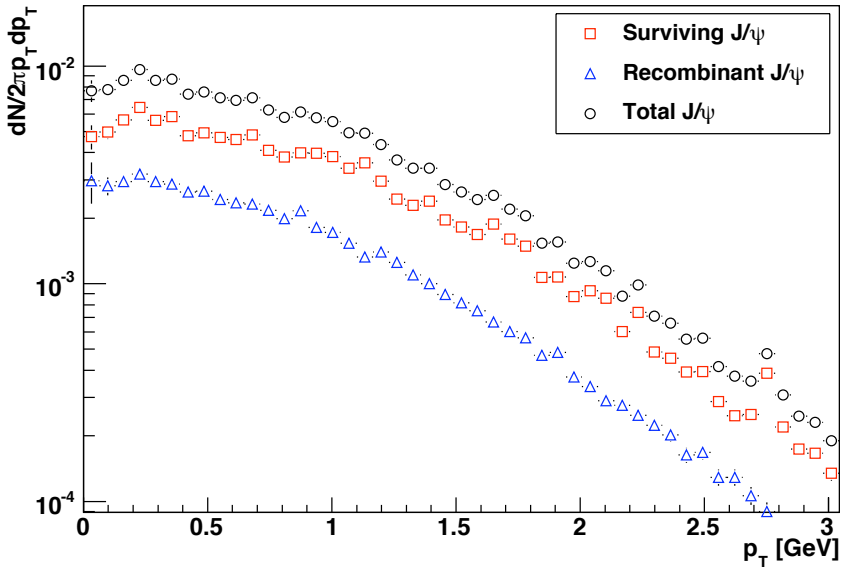

Figure 4.9: (Color online.) The surviving and recombinant J/ψ yields versus p_t.

Chapter 5

Path integrals for quantum Brownian motion and quarkonium

We will outline how the imaginary-time propagator with periodicity $\beta = 1/T$ can be determined for quarkonium systems interacting with a heat bath. In Section 5.1, we review the reduced density matrix, apply the model of Caldeira and Leggett for quantum Brownian motion to imaginary time, and then describe briefly path-integral Monte Carlo techniques for calculating this reduced density matrix. In Section 5.2, we show how the imaginary-time propagator for charmonium may be calculated to high accuracy with these techniques, for any potential or drag coefficient, and we show the results for $G(\tau, T)$ for the vector channel at temperatures just above the deconfinement transition.

Not many before have considered the effect of the medium on heavy quark and quarkonium Euclidean correlators calculated on the lattice. Current work by Beraudo et al. [82] does consider the medium effect on heavy quark correlators. Starting from the QCD Lagrangian, they make the HTL approximation for the heavy quark's interaction with the light degrees of freedom at finite temperature, and then they integrate these degrees of freedom out. The focus of our work is on a heavy particle interacting quite strongly with the medium, as suggested by calculations taking advantage of gauge-gravity duality [17]. We show how the Lagrangian for a particle interacting strongly with a heat bath can be renormalized so that functional integration is well-defined, and where analytic results are possible.

5.1 The path integral form for the reduced density matrix of a dissipative system

For an excellent review of the functional integral approach to quantum Brownian motion, in both imaginary and real time, see [83]. For a briefer discussion of these ideas and how they apply to quarkonium, see [84]. These results are discussed in generality, and shown to arise from the Schwinger-Keldysh contour integral for a heavy quark's real-time partition function, by Son and Teaney [85]. These systems can be studied with approaches besides the path-integral formulation, and the study of quantum Brownian motion, in terms of a partial differential equation for the density matrix, has been studied by Hu, Paz, and Zhang [86, 87].

5.1.1 The reduced density matrix

Without loss of generality, consider a system consisting of a heavy particle of mass M which we will call the system, minimally coupled to a harmonic oscillator of mass m.

$$\begin{aligned} L &= L_S + L_I; \\ L_S &= \frac{1}{2}M\dot{x}^2 - V(x), \\ L_I &= \frac{1}{2}m\dot{r}^2 - \frac{1}{2}m\omega^2 r^2 - Cxr. \end{aligned} \tag{5.1}$$

We analytically continue this Lagrangian to $\tau = it$.

$$\begin{aligned} S_S^E[x] &= \int_0^\beta \left[\frac{1}{2}M\dot{x}^2 + V(x)\right], \\ S_I^E[x,r] &= \int_0^\beta \left[\frac{1}{2}m\dot{r}^2 + \frac{1}{2}m\omega^2 r^2 + Cxr\right] d\tau \end{aligned} \tag{5.2}$$

We can simplify this Lagrangian by making a change of variables. We subtract the particular solution to the classical equations of motion as determined by Eq. 5.2.

$$\begin{aligned} r(\tau) &\equiv r'(\tau) + \frac{C}{m\omega}\int_0^\tau d\tau' x(\tau') \sinh\left[\omega(\tau - \tau')\right] \\ &\equiv r'(\tau) + A[x,\tau] \end{aligned} \tag{5.3}$$

In terms of the shifted coordinate r' the Euclidean action becomes that of a simple harmonic oscillator:

$$\begin{aligned} S_I^E[x,r] &= \int_0^\beta \left[\frac{1}{2}m\dot{r}'^2 + \frac{1}{2}m\omega^2 r'^2 + \frac{1}{2}Cx(\tau)A[x,\tau]\right] d\tau \\ &\quad + m\dot{A}[x,\beta]\left(r'(\beta) + \frac{1}{2}A[x,\beta]\right) \\ &\equiv S_I'^E[x,r']. \end{aligned} \tag{5.4}$$

As always, the propagator of a system for imaginary time $\beta = -i/T$ gives matrix elements of the thermal density operator. In our example, the density matrix has 4 indices, 2 for each degree of freedom of the system. In the example given above the density matrix is given as

$$\rho(x_i, r_i; x_f, r_f; \beta) = \int_{x(0)=x_i}^{x(\beta)=x_f} \mathcal{D}x \int_{r(0)=r_i}^{r(\beta)=r_f} \mathcal{D}r \exp\left(-S_S^E[x] - S_I^E[x,r]\right). \tag{5.5}$$

If we were never interested in measurements of the degree of freedom r, we could take the trace over the indices corresponding to this degree of freedom, and work with a density operator with only two indices. With this in mind, we define the *reduced density matrix*:

$$\rho_{red}(x_i, x_f, \beta) \equiv \int dr \rho(x_i, r; x_f, r; \beta). \tag{5.6}$$

In the next section it will be the only operator practical for calculating thermal averages.

For the system defined by Eq. 5.1, we can now write a path-integral description of the reduced density matrix,

$$\begin{aligned} \rho_{red}(x_i, x_f, \beta) &= \int dr \int \mathcal{D}x\, \mathcal{D}r' \, \exp\left(-S_S^E[x] - S_I^E[x,r']\right) \\ &= \int \mathcal{D}x \exp\left(-S_x^E[x]\right) \int dr \int \mathcal{D}r' \exp\left(-S_I'^E[x,r']\right) \end{aligned} \tag{5.7}$$

where we integrate over paths with endpoints $x(0) = x_i$, $x(\beta) = x_f$, $r'(0) = r$, and $r'(\beta) = r - A[x,\beta]$. The final step in 5.7 allows the integral over the paths $r'(\tau)$ to be performed independently of the integral over $x(\tau)$. Using Eq. 5.4,

a simple Gaussian integral yields

$$\begin{aligned}\rho_{red}(x_i, x_f, \beta) &= \int_{x(0)=x_i}^{x(\beta)=x_f} \mathcal{D}x \exp\Big\{ - S_S^E[x] \\ &+ \sum_i \frac{C_i^2}{2m\omega_i \sinh(\frac{\omega_i \beta}{2})} \\ &\times \int_0^\beta d\tau \int_0^\tau ds\; x(\tau)x(s) \cosh\left[\omega_i \left(\tau - s - \beta/2\right)\right] \Big\}, \quad (5.8)\end{aligned}$$

where the summation is introduced because we have generalized this to a system where a heavy particle interacts with a bath of simple harmonic oscillators. This is now the path integral form for the reduced density matrix. This is analogous to the idea of influence functionals, worked out for real-time propagators many years ago [88].

5.1.2 Making a dissipative system

Any finite quantum-mechanical system is reversible and therefore inappropriate for describing Brownian motion. One might find it intuitive that if the bath of harmonic oscillators were taken to an infinite limit, it would be "large enough" so that energy from the heavy particle could dissipate into the system and never return. This intuition was proven to be true by the authors of [89], who considered the real-time evolution of the density matrix for our system and showed that when the bath of harmonic oscillators is determined by the continuous density of states

$$C^2(\omega)\rho_D(\omega) = \begin{cases} \frac{2m\eta\omega^2}{\pi} & \text{if } \omega < \Omega \\ 0 & \text{if } \omega > \Omega \end{cases} \quad (5.9)$$

the force autocorrelator for the heavy particle is proportional to $\delta(t - t')$ at high temperatures. In this "white noise" limit, the density matrix describes an ensemble of particles interacting according to the Langevin equation, which has been used to describe Brownian motion for a long time. It is a stochastic differential equation, is irreversible, and evolves any ensemble towards the thermal phase space distribution.

We now take this density of states and substitute it into Eq. 5.8

$$\begin{aligned}\rho_{red}(x_i,x_f,\beta) &= \int_{x(0)=x_i}^{x(\beta)=x_f}\mathcal{D}x\exp\Bigg\{-S_S^E[x]\\ &+ \frac{\eta}{\pi}\int_0^\Omega d\omega\int_0^\beta d\tau\int_0^\tau ds\\ &\times\ x(\tau)x(s)\frac{\omega\cosh\left[\omega(\tau-s-\beta/2)\right]}{\sinh(\frac{\omega\beta}{2})}\Bigg\}. \end{aligned}\tag{5.10}$$

The divergences of this action can be isolated by integrating by parts twice

$$\begin{aligned}&\int_0^\Omega d\omega\int_0^\beta d\tau\int_0^\tau ds\ x(\tau)x(s)\frac{\omega\cosh\left[\omega(\tau-s-\beta/2)\right]}{\sinh(\frac{\omega\beta}{2})}\\ =\ &\Omega\int_0^\beta d\tau\ (x(\tau))^2-\frac{1}{2}(x_i-x_f)^2\ln(M\Omega/\eta)\frac{\cosh(\Omega\beta/2)-1}{\sinh(\Omega\beta/2)}\\ &-\frac{1}{2}(x_i-x_f)^2\left[\gamma_E+\ln\left(\frac{\eta\beta}{\pi M}\right)\right]\\ &+(x_i-x_f)\int_0^\beta d\tau\ \dot{x}(\tau)\ \mathrm{lnsin}\left(\frac{\pi\tau}{\beta}\right)\\ &+\int_0^\beta d\tau\int_0^\tau ds\ \dot{x}(\tau)\dot{x}(s)\ \mathrm{lnsin}\left(\frac{\pi(\tau-s)}{\beta}\right), \end{aligned}\tag{5.11}$$

where $\mathrm{lnsin}(x)\equiv\ln\left[\sin(x)\right]$ and γ_E is the Euler-Mascheroni constant. The first two terms on the right-hand side correspond to a renormalization of the potential for the heavy particle, always necessary when considering the interaction of a particle with infinitely many additional degrees of freedom. They are temperature-independent in the limit of large Ω, and may be introduced as temperature-independent modifications of the Lagrangian for the particle. The final three terms are finite and well-behaved, and have been evaluated in the limit $\Omega\to\infty$. The final form for the reduced density matrix becomes

$$\begin{aligned}\rho_{red}(x_i,x_f,\beta) &= \int_{x(0)=x_i}^{x(\beta)=x_f}\mathcal{D}x\ \exp\Bigg\{-S_S^E[x]-\frac{\eta}{2\pi}(x_i-x_f)^2\left[\gamma_E+\ln\left(\frac{\eta\beta}{\pi M}\right)\right]\\ &+\ \frac{\eta}{\pi}(x_i-x_f)\int_0^\beta d\tau\ \dot{x}(\tau)\ \mathrm{lnsin}\left(\frac{\pi\tau}{\beta}\right)\\ &+\ \frac{\eta}{\pi}\int_0^\beta d\tau\int_0^\tau ds\ \dot{x}(\tau)\dot{x}(s)\ \mathrm{lnsin}\left(\frac{\pi(\tau-s)}{\beta}\right)\Bigg\}. \end{aligned}\tag{5.12}$$

In summary, we have determined an expression for the reduced density matrix of a system (consisting of a massive particle in a potential) interacting with a bath of oscillators. The coupling to the bath has been chosen in order to reproduce the results of classical Brownian motion in the high temperature limit. We have taken care to make the term in the exponential finite, by isolating the divergences through integration by parts. This is important for path integral Monte Carlo simulation to be possible for this functional integral.

5.1.3 Example: The otherwise free particle

The reduced density matrix for a particle interacting with such a bath can be determined analytically for the otherwise free particle ($V_R(x) = 0$). First, write an arbitrary path as an expansion around the classical solution

$$\begin{aligned} x(\tau) &= x_{cl}(\tau) + \xi(\tau); \\ x_{cl}(\tau) &\equiv x_i + (x_f - x_i)\tau/\beta, \\ \xi(\tau) &\equiv \sum_{n=1}^{\infty} c_n \sin\left(\frac{n\pi\tau}{\beta}\right). \end{aligned} \tag{5.13}$$

One can find an analytic solution by substituting this into Eq. 5.12 . We skip the details: after evaluating numerous integrals using contour integration, and then changing variables for the integration over the even Fourier coefficients, we find the reduced density matrix

$$\begin{aligned} \rho_{red}(x_i, x_f, \beta) &= \sqrt{\frac{M}{2\pi\beta} + \frac{\eta}{2\pi^2}\left[\log(2) + \gamma_E + \Psi\left(1 + \frac{\eta\beta}{2\pi M}\right)\right]} \\ &\times \exp\left\{ -\left[\frac{M}{2\beta} + \frac{\eta}{2\pi}\left[\log\left(\frac{\eta\beta}{2\pi M}\right) - \Psi\left(1 + \frac{\eta\beta}{2\pi M}\right)\right]\right] \right. \\ &\times \left. (x_i - x_f)^2 \right\}, \end{aligned} \tag{5.14}$$

where $\Psi(x)$ is the digamma function and the overall normalization is determined by analytic continuation of β and requiring the propagator to conserve probability for purely imaginary β. One interesting physical result is easily obtained from the Fourier transform of the reduced density matrix

$$\left\langle p^2 \right\rangle = \frac{M_{eff}}{\beta}, \quad M_{eff} = M + \frac{\eta\beta}{\pi}\left[\log\left(\frac{\eta\beta}{2\pi M}\right) - \Psi\left(1 + \frac{\eta\beta}{2\pi M}\right)\right]. \tag{5.15}$$

5.1.4 The path-integral Monte Carlo algorithm for the reduced density matrix

Obtaining the analytic result for our reduced density matrix was reasonable for the otherwise free particle. For the simple harmonic oscillator, the analytic result exists but has a rather complicated expression. For the potentials which describe quarkonium spectroscopy with some precision, analytic work becomes entirely impractical. We would like to use numerical simulation to obtain reliable estimates of reduced density matrices and Euclidean correlators.

The most natural numerical approach for the formalism we adopted is path-integral Monte Carlo (PIMC). For an excellent review of the technique, see the review of D. M. Ceperley [90]. Paths are either sampled according to a Metropolis algorithm determined by the action of interest, or sampled from some convenient distribution which samples the entire space of paths with some weight. For our work with a single degree of freedom, we found that sampling a convenient distribution (in our case, the distribution of paths determined by $\exp(-S_{free}[x])$) to be sufficient, which is easily sampled for any discretization of the path with a bisection method. When sampling the space of paths, the next step is to determine an estimate for the action of each path. For our case, the primitive action with the simplest integration of the new dissipative terms is sufficient. Once this is determined, any correlator can be calculated by sampling paths and making weighted averages.

5.2 Quarkonium as an open quantum system

We should now apply this functional integral to the problem of quarkonium at temperatures above deconfinement. To this end, let us rework the Euclidean correlators calculated on the lattice to a form with which we can calculate.

For a given channel, the two-point Euclidean correlator for a composite mesonic operator is given by

$$\begin{aligned} G(\tau, T) &= \int d^3x \left\langle J_\Omega(\mathbf{x}, \tau) J_\Omega(\mathbf{0}, 0) \right\rangle_\beta , \\ J_\Omega(\mathbf{x}, \tau) &= \bar{\psi}(\mathbf{x}, \tau) \Omega \psi(\mathbf{x}, \tau), \end{aligned} \tag{5.16}$$

where $\Omega = 1, \gamma^0, \gamma^\mu, \gamma^0\gamma^\mu$ determine the mesonic channel to be scalar, pseudo-scalar, vector, or pseudo-vector, respectively.

For now, consider only the vector channel (the following arguments must be modified for the scalar and pseudo-vector channels). In order to switch to a first-quantization approach for the energy range where a potential model would

be appropriate, think of this correlator as being the sum of the expectation values of an operator over all of the states in the Fock space of N-particle mesonic systems, with each expectation value entering the sum weighted by the state's Boltzmann factor. One term in this sum, of course, is the "vacuum" expectation value

$$\langle 0|J^{\mu}(\mathbf{x},\tau)J_{\mu}(\mathbf{0},0)|0\rangle = \langle \mu,\mathbf{x};\tau|\mu,\mathbf{0};0\rangle_{\text{light}}\,, \tag{5.17}$$

where the subscript represents that the trace is still taken over all of the light degrees of freedom in QCD.

The right-hand side of Equation 5.17 represents an important step: by decomposing the mesonic operators into products of creation and annihilation operators, the vacuum expectation value can be related to the overlap of two one-particle states. Also, note here that since expectation values of the higher states enter into the thermal average multiplied by factors which are roughly powers of $\exp(-2M_Q/T)$, the vacuum expectation value dominates the thermal average in the limit $M \gg T$. Therefore, we have identified the leading contribution to the correlator in the vector channel.

The trace over the light degrees of freedom is of course the central problem of QCD, and no analytic result exists. However, in the infinite mass limit, this has been computed on the lattice as the expectation value of two Polyakov loops [22]. The dissipative effects on this propagator have been studied, as we noted previously, by gauge-gravity duality. Our ansatz here is that these results describe well the dynamics of sufficiently heavy quarks.

The path integral we wish to evaluate can be written in terms of relative and absolute coordinates as

$$\begin{aligned}
\langle \mathbf{x},\mathbf{x};\tau|\mathbf{0},\mathbf{0};0\rangle \quad &= \quad \int \mathcal{D}\mathbf{X}\exp\left\{-\int_0^{\beta} d\tau M\dot{\mathbf{X}}^2\right. \\
&+ \quad \left.\frac{2\eta}{\pi}\int_0^{\beta} d\tau\int_0^{\tau} ds\;\dot{\mathbf{X}}(\tau)\dot{\mathbf{X}}(s)\;\mathrm{lnsin}\left(\frac{\pi}{\beta}(\tau-s)\right)\right\} \\
\times\int \mathcal{D}\mathbf{x}_{rel} \quad &\exp \quad \left\{-\int_0^{\beta} d\tau\left[\frac{1}{4}M\dot{\mathbf{x}}_{rel}^2 + V(\mathbf{x}_{rel})\right]\right. \\
+\frac{\eta}{2\pi}\int_0^{\beta} d\tau\int_0^{\tau} \quad ds \quad &\left.\dot{\mathbf{x}}_{rel}(\tau)\dot{\mathbf{x}}_{rel}(s)\;\mathrm{lnsin}\left(\frac{\pi}{\beta}(\tau-s)\right)\right\},
\end{aligned} \tag{5.18}$$

where the functional integration are over all paths satisfying $\mathbf{X}(0)=\mathbf{0}$, $\mathbf{X}(\tau)=\mathbf{x}$, $\mathbf{X}(\beta)=\mathbf{0}$, $\mathbf{x}_{rel}(0)=\mathbf{0}$, $\mathbf{x}_{rel}(\tau)=\mathbf{0}$, and $\mathbf{x}_{rel}(\beta)=\mathbf{0}$.

The right-hand side of Equation 5.18 can now be calculated, for any potential, with a PIMC simulation. We use the Cornell potential for the interaction

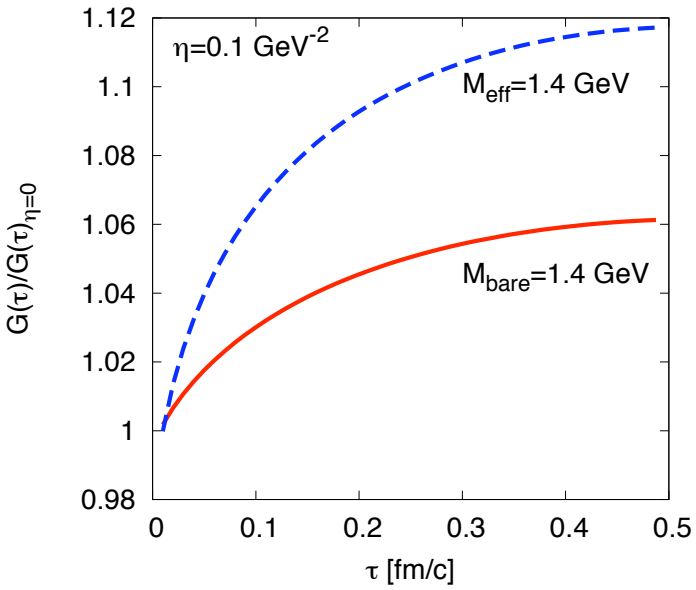

Figure 5.1: $G(\tau)/G_{\eta=0}$ evaluated for $\eta = 0.1$ GeV^{-2} at $T = 1.2T_c$.

between the heavy quarks.

To obtain $G(\tau)$, the first term on the right-hand side of Eq. 5.18 is integrated with respect to $\mathbf{X}$, yielding the diagonal value for the free-particle reduced density matrix which is independent of τ. In Figure 5.1 we show the mesonic correlator as a function of τ at $T = 1.2T_c$. We have chosen a representative value of $\eta = 0.1$ GeV^{-2} and show results for fixed bare and effective charm mass.

Clearly, dissipative effects due to the medium change the mesonic correlators measured in lattice simulations. Also, these effects are not trivial: holding the effective charm mass fixed but varying η still leads to changes in the mesonic correlators. The next step is to perform spectral analysis of these correlators to examine how dissipation affects the spectral function for this correlator. From here, the dissipative effects can be included in heavy-ion phenomenology.

Chapter 6

Conclusions and future work

Typically in particle physics, the rate for the scattering of an N-particle state into another is determined from the square of the matrix element whose indices are the initial and final states, where these states are in the momentum basis. This makes perfect sense in high-energy experiments, where the incoming and outgoing states are basically each 2-particle momentum eigenstates and the matrix element can be expanded in terms of a small coupling. Such an approach, however, seems entirely inappropriate for quarkonium formed in a heavy-ion collision, whose constituent quarks are localized in position relative to the surrounding medium and are strongly coupled both to the medium and each other. Non-perturbative techniques and experiment both suggest that quarkonium rapidly thermalizes and interacts strongly with the medium. The most reasonable approach for explaining the observables is to describe quarkonium with a reduced density matrix, whose evolution is determined by a potential *and* a drag coefficient which are both determined non-perturbatively.

To put it another way: as far back as Fermi, physicists understood the utility of describing collisions yielding very high multiplicities with hydrodynamics. The full utility of this approach is realized in ultrarelativistic heavy-ion collisions, where nearly ideal flow agrees quite well with most observables. If one wanted to understand the dynamics of particles that are heavy compared to the surrounding medium, during the time when the whole medium is described with hydrodynamics, then one should look no further than Einstein's description of Brownian motion for an appropriate model. This is exactly how Moore and Teaney described single charm quarks during the hydrodynamical phase. My work simply extended theirs to charmonium, making the simplest assumption for the white noise: that the white noises experienced by each constituent quark be uncorrelated. In this way, my work has been extremely conservative, and yet, it explains both thermalization in relative yields and the suppression pattern with no fine-tuning, besides a great deal of sensitivity

to the freeze-out temperature T_c.

A great deal of work remains to be done, and I break up my description into three parts: phenomenology, comparing the model with lattice results, and better determination of quarkonium dynamics.

Concerning phenomenology: while my model explains well the R_{AA} for the yield of J/ψ as a function of number of participants, so do various other models. I will write here, however, that my model has only one "crank": the value chosen for the critical temperature below which the transport of the heavy quarks ceases, while many other models have many cranks whose sensitivity are not well-advertised. Of course, it is problematic when many competing models with, in some cases, contradicting physical processes can all explain data. One important observable which may change this situation is the formation of $b\bar{c}$ "atomic" mesons in heavy-ion collisions. These mesons, extremely rare in proton-proton collisions, might be greatly enhanced during a deconfined phase [92]. The Langevin-with-interaction model predicts that most of the yield of J/ψ, even in central gold-gold collisions at the RHIC, comes from the "surviving" component, not the "recombinant" component. Similarly, the $b\bar{c}$ states at the RHIC, which predicted to be produced almost entirely recombinantly, might have a smaller yield at the RHIC than currently expected in models where recombinant production is significant, if the Langevin-with-interaction approach is to be believed. A quantitative prediction concerning this yield is within reach and will be determined soon.

Also important is the phenomenology of heavy-ion collisions at the LHC. Here, high densities of $\bar{c}c$ pairs start to make averaging over the possible pairings of quarks and anti-quarks into quarkonium difficult. Simulation of $\bar{c}c$ pairs at the LHC will have to be coupled with sampling of pairings using the Metropolis algorithm in order to predict the (possibly large) recombinant contribution to the final yields of charmonium at the LHC.

More work must also be done in making contact between the Langevin-with-interaction model and the important results from lattice QCD. As shown in Chapter 5, imaginary-time propagators calculated using path-integral Monte Carlo can be related to quarkonium correlation functions calculated using the lattice. However, these imaginary-time propagators need to be spectrally analyzed, most likely using Bayesian statistics, to obtain the Fourier transform of the *real-time* quarkonium correlation functions. In this way, the spectral function obtained can be used in the proper, non-relativistic range, with the perturbative QCD result for the spectral density replacing our result at large ω and with the low-frequency component due to heavy-quark diffusion added as well. This "processed" spectral density will yield the imaginary-time correlation functions that can finally be compared with lattice data. This difficult

process is necessary to make real comparisons between lattice data and the results of our model with different diffusion coefficients and heavy-quark potentials, so that quantitative statements may be made about the behavior of quarkonium at temperatures above deconfinement.

Bayesian analysis of lattice correlation functions has perhaps been slightly undersold. Whenever some data set X depends on a spectral density ρ_i, usually discretized over some continuous variable (in this case, ω), the maximal entropy method finds a solution for ρ_i, which is usually under-determined, by minimizing a function with a χ^2 term and the Shannon entropy term:

$$f[X, \rho_i] = \chi^2[X, \rho_i] + \lambda \sum_i \rho_i \ln \rho_i, \tag{6.1}$$

where λ is also varied to achieve a realistic value for χ^2. Often times, this function has justified using the principle of maximal entropy, which basically states that if you know nothing about a coin, you should assume that the coin is equally weighted for any resulting outcome. Many people find this assumption unpalatable, perhaps rightly so. However, what people should also notice is that the Shannon entropy term is an assumption on the smoothness of the spectral density, a perfectly reasonable assumption considering that every input to the action for this system is a continuous function.

Another interesting route here would be to calculate the evolution of the reduced density matrix of Caldeira and Leggett [89](and corrected by Grabert, Schramm, and Ingold [83]) using path-integral Monte Carlo. The conventional wisdom that nuclear theorists develop from our experience with lattice QCD is that it is impossible to calculate sums over all paths numerically in real-time, due to the fact that $\exp(iS)$ is rapidly oscillating and nowhere decaying. However, while it is definitely true that these oscillating integrals are impossible numerically with the many degrees of freedom for a field, this is actually not true for systems with only a few degrees of freedom. In chemical physics, a common technique is to split real-time path integrals into short-time propagators and to use approximations to these propagators, see for example [93]. It would be of some general interest to develop numerical codes which calculate the real-time evolution of these reduced density matrices in this way.

Finally, the dynamics of quarkonium above deconfinement needs to be investigated starting from the first principles of QCD. One part of this will surely be using lattice QCD to calculate different quarkonium correlation functions, as well as some of the ones discussed here to higher precision. Also, there exists a great deal of work in the "AdS/QCD" model, which leads to correlation functions which have some of the same behavior as those in QCD, and a great deal of work has been done examining quarkonium using these models

[94]. While the lattice remains the best source for quantitative first-principle results, perhaps gauge/gravity duality will finally provide intuitive pictures for the dynamics of quarkonium and with it, a better understanding of the emergent properties of QCD.

Bibliography

[1] T. Schafer and E. V. Shuryak, Rev. Mod. Phys. **70**, 323 (1998) [arXiv:hep-ph/9610451].

[2] G. 't Hooft, Nucl. Phys. B **190**, 455 (1981).

[3] C. Amsler *et al.* [Particle Data Group], Phys. Lett. B **667**, 1 (2008).

[4] T. Appelquist, A. De Rujula, H. D. Politzer and S. L. Glashow, Phys. Rev. Lett. **34**, 365 (1975).

[5] E. Eichten, K. Gottfried, T. Kinoshita, J. B. Kogut, K. D. Lane and T. M. Yan, Phys. Rev. Lett. **34**, 369 (1975) [Erratum-ibid. **36**, 1276 (1976)].

[6] E. Eichten, K. Gottfried, T. Kinoshita, K. D. Lane and T. M. Yan, Phys. Rev. D **17**, 3090 (1978) [Erratum-ibid. D **21**, 313 (1980)].

[7] K. H. Ackermann *et al.* [STAR Collaboration], Phys. Rev. Lett. **86**, 402 (2001) [arXiv:nucl-ex/0009011].

[8] J. Lettesier and J. Rafelski, *Hadrons and Quark-Gluon Plasma*, Cambridge University Press, 2002, p. 316-370

[9] K. Adcox *et al.* [PHENIX Collaboration], Phys. Lett. B **561**, 82 (2003) [arXiv:nucl-ex/0207009].

[10] B. Alessandro *et al.* [NA50 Collaboration], Eur. Phys. J. C **39**, 335 (2005) [arXiv:hep-ex/0412036].

[11] E. V. Shuryak, Phys. Lett. B **78**, 150 (1978) [Sov. J. Nucl. Phys. **28**, 408.1978 YAFIA,28,796 (1978 YAFIA,28,796-808.1978)].

[12] T. Matsui and H. Satz, Phys. Lett. B **178**, 416 (1986).

[13] S. Caron-Huot and G. D. Moore, Phys. Rev. Lett. **100**, 052301 (2008) [arXiv:0708.4232 [hep-ph]].

[14] J. M. Maldacena, Adv. Theor. Math. Phys. **2**, 231 (1998) [Int. J. Theor. Phys. **38**, 1113 (1999)] [arXiv:hep-th/9711200].

[15] E. Witten, Adv. Theor. Math. Phys. **2**, 253 (1998) [arXiv:hep-th/9802150].

[16] S. S. Gubser, Phys. Rev. D **74**, 126005 (2006) [arXiv:hep-th/0605182].

[17] J. Casalderrey-Solana and D. Teaney, Phys. Rev. D **74**, 085012 (2006) [arXiv:hep-ph/0605199].

[18] A. Adare *et al.* [PHENIX Collaboration], Phys. Rev. Lett. **98**, 172301 (2007) [arXiv:nucl-ex/0611018].

[19] G. D. Moore and D. Teaney, Phys. Rev. C **71**, 064904 (2005) [arXiv:hep-ph/0412346].

[20] M. Creutz, *Quarks, gluons and lattices*, 1983, Cambridge Monographs on Mathematical Physics

[21] P. Petreczky and D. Teaney, Phys. Rev. D **73**, 014508 (2006) [arXiv:hep-ph/0507318].

[22] O. Kaczmarek, F. Karsch, P. Petreczky and F. Zantow, Phys. Lett. B **543**, 41 (2002) [arXiv:hep-lat/0207002].

[23] F. Karsch, M. T. Mehr and H. Satz, Z. Phys. C **37**, 617 (1988).

[24] K. Dusling and C. Young, arXiv:0707.2068 [nucl-th].

[25] E. V. Shuryak and I. Zahed, Phys. Rev. D **70**, 054507 (2004) [arXiv:hep-ph/0403127].

[26] A. Jakovac, P. Petreczky, K. Petrov and A. Velytsky, Phys. Rev. D **75**, 014506 (2007) [arXiv:hep-lat/0611017].

[27] A. Mocsy and P. Petreczky, J. Phys. G **35**, 104154 (2008).

[28] H. Liu, K. Rajagopal and U. A. Wiedemann, Phys. Rev. Lett. **98**, 182301 (2007) [arXiv:hep-ph/0607062].

[29] K. Dusling, J. Erdmenger, M. Kaminski, F. Rust, D. Teaney and C. Young, JHEP **0810**, 098 (2008) [arXiv:0808.0957 [hep-th]].

[30] F. Reif, *Fundamentals of statistical and thermal physics*, McGraw-Hill and Company, 1965, p. 560.

[31] Richard Durrett, *Stochastic calculus: a practical introduction*, Boca Raton: CRC Press, 1996.

[32] P. B. Arnold, Phys. Rev. E **61**, 6091 (2000) [arXiv:hep-ph/9912208].

[33] B. Andersson, G. Gustafson and C. Peterson, Phys. Lett. B **71**, 337 (1977). T. Sjöstrand, S. Mrenna and P. Skands, JHEP **0605**, 026 (2006)

[34] H. Sorge, E. V. Shuryak and I. Zahed, Phys. Rev. Lett. **79**, 2775 (1997)

[35] A. Andronic, P. Braun-Munzinger, K. Redlich and J. Stachel, Phys. Lett. B **571**, 36 (2003) [arXiv:nucl-th/0303036].

[36] A. Adare *et al.* [PHENIX Collaboration], Phys. Rev. Lett. **98**, 232301 (2007) [arXiv:nucl-ex/0611020].

[37] C. Young and E. Shuryak, Phys. Rev. C **79**, 034907 (2009) [arXiv:0803.2866 [nucl-th]].

[38] D. Teaney, J. Lauret and E. V. Shuryak, arXiv:nucl-th/0110037.

[39] C. Young and E. Shuryak, arXiv:0911.3080 [nucl-th].

[40] E. Fermi, Prog. Theor. Phys. **5**, 570 (1950).

[41] L. D. Landau, Izv. Akad. Nauk Ser. Fiz. **17**, 51 (1953).

[42] K. Dusling and D. Teaney, Phys. Rev. C **77**, 034905 (2008) [arXiv:0710.5932 [nucl-th]].

[43] C. N. Yang and R. L. Mills, Phys. Rev. **96**, 191 (1954).

[44] M. Gell-Mann and Y. Ne'eman, *The Eightfold Way*, Benjamin, 1964

[45] D. J. Gross and F. Wilczek, Phys. Rev. D **8**, 3633 (1973).

[46] H. D. Politzer, Phys. Rept. **14**, 129 (1974).

[47] M. Creutz, Phys. Rev. D **21**, 2308 (1980).

[48] R. J. Glauber, Phys. Rev. **100**, 242 (1955).

[49] T. Lappi and R. Venugopalan, Phys. Rev. C **74**, 054905 (2006) [arXiv:nucl-th/0609021].

[50] S. S. Gubser, S. S. Pufu and A. Yarom, JHEP **0911**, 050 (2009) [arXiv:0902.4062 [hep-th]].

[51] E. Iancu and R. Venugopalan, arXiv:hep-ph/0303204.

[52] J. D. Bjorken, Phys. Rev. D **27**, 140 (1983).

[53] Randall J. LeVeque, *Finite Volume Methods for Hyperbolic Problems*, Cambridge University Press, 2002

[54] C. Bernard *et al.*, Phys. Rev. D **75**, 094505 (2007) [arXiv:hep-lat/0611031].

[55] V. Emel'yanov, A. Khodinov, S. R. Klein and R. Vogt, Phys. Rev. C **56**, 2726 (1997) [arXiv:nucl-th/9706085].

[56] J. A. Appel, Ann. Rev. Nucl. Part. Sci. **42**, 367 (1992).

[57] K. Tuchin, Nucl. Phys. A **830**, 243C (2009) [arXiv:0907.1604 [nucl-th]].

[58] P. Braun-Munzinger and J. Stachel, Phys. Lett. B **490**, 196 (2000).

[59] B. B. Back *et al.*, Nucl. Phys. A **757**, 28 (2005)

[60] I. Arsene *et al.* [BRAHMS Collaboration], Nucl. Phys. A **757**, 1 (2005)

[61] S. S. Adler *et al.* [PHENIX Collaboration], Phys. Rev. Lett. **96**, 012304 (2006)

[62] X. Dong, AIP Conf. Proc. **828**, 24 (2006) [Nucl. Phys. A **774**, 343 (2006)]

[63] O. Kaczmarek, S. Ejiri, F. Karsch, E. Laermann and F. Zantow, Prog. Theor. Phys. Suppl. **153**, 287 (2004)

[64] F. Karsch, D. Kharzeev and H. Satz, Phys. Lett. B **637**, 75 (2006)

[65] D. Kharzeev and M. Nardi, Phys. Lett. B **507**, 121 (2001)

[66] A. Adare *et al.* [PHENIX Collaboration], Phys. Rev. Lett. **98**, 232301 (2007)

[67] S. Digal, P. Petreczky and H. Satz, Phys. Rev. D **64**, 094015 (2001)

[68] A. Adare *et al.* [PHENIX Collaboration], arXiv:0802.0050 [hep-ex].

[69] J. Liao and E. Shuryak, Phys. Rev. C **75**, 054907 (2007)

[70] M. N. Chernodub and V. I. Zakharov, Phys. Rev. Lett. **98**, 082002 (2007)

[71] J. Liao and E. Shuryak, Phys. Rev. C **77**, 064905 (2008)

[72] J. Liao and E. Shuryak, arXiv:0804.4890 [hep-ph].

[73] C. Silvestre and f. t. P. Collaboration, arXiv:0808.2925 [nucl-ex].

[74] V. Greco, C. M. Ko and R. Rapp, Phys. Lett. B **595**, 202 (2004)

[75] L. Grandchamp and R. Rapp, Nucl. Phys. A **709**, 415 (2002).

[76] S. S. Adler *et al.* [PHENIX Collaboration], Phys. Rev. Lett. **94**, 082301 (2005).

[77] One can find the program at http://www-linux.gsi.de/ misko/ .

[78] http://www.int.washington.edu/talks/WorkShops/ , presented by M. Leitch at the Joint CATHIE-INT mini-program Quarkonium in Hot Media: From QCD to Experiment

[79] X. Zhao and R. Rapp, Eur. Phys. J. C **62**, 109 (2009).

[80] C. P. Herzog, A. Karch, P. Kovtun, C. Kozcaz and L. G. Yaffe, JHEP **0607**, 013 (2006) [arXiv:hep-th/0605158].

[81] A. Mocsy and P. Petreczky, PoS **LAT2007**, 216 (2007) [arXiv:0710.5205 [hep-lat]].

[82] A. Beraudo, J. P. Blaizot, G. Garberoglio and P. Faccioli, Nucl. Phys. A **830**, 319C (2009) [arXiv:0907.1797 [hep-ph]].

[83] H. Grabert, P. Schramm and G. L. Ingold, Phys. Rept. **168**, 115 (1988).

[84] C. Young at the INT-CATHIE Joint mini-program "Quarkonium in hot media: from QCD to Experiment," June 22, 2009

[85] D. T. Son and D. Teaney, JHEP **0907**, 021 (2009) [arXiv:0901.2338 [hep-th]].

[86] B. L. Hu, J. P. Paz and Y. h. Zhang, Phys. Rev. D **45**, 2843 (1992).

[87] B. L. Hu, J. P. Paz and Y. Zhang, Phys. Rev. D **47**, 1576 (1993).

[88] R.P. Feynman and A.R. Hibbs, *Quantum Mechanics and Path Integrals* (McGraw-Hill, New York, 1965)

[89] A. O. Caldeira and A. J. Leggett, Physica **121A**, 587 (1983).

[90] D. M. Ceperley, *Reviews of Modern Physics* Vol. 67, No. 2, April 1995

[91] E. Shuryak, [arXiv:0903.3734 [nucl-th]].

[92] M. Schroedter, R. L. Thews and J. Rafelski, Phys. Rev. C **62**, 024905 (2000) [arXiv:hep-ph/0004041].

[93] Xin Ma, Donald J. Kouri and David K. Hoffman, Chem. Phys. Lett. **208**, Issues 3-4, 207(1993).

[94] M. Mia, K. Dasgupta, C. Gale and S. Jeon, Phys. Rev. D **82**, 026004 (2010) [arXiv:1004.0387 [hep-th]].

Appendices

Coalescence Probability

After all distributions at the end of the QGP era are determined, the next step is to calculate the probabilities of it materializing as a particular charmonium state.

One approach is based on the Wigner probability distribution. For any wavefunction $\psi(\mathbf{x})$,

$$W_\psi(\mathbf{x},\mathbf{p}) = \frac{1}{\pi^3}\int d^3y \psi^*(\mathbf{x}+\frac{\mathbf{y}}{2})\psi(\mathbf{x}-\frac{\mathbf{y}}{2})e^{i\mathbf{p}\cdot\mathbf{y}}. \tag{2}$$

The wave function for J/ψ was easily calculated numerically and then fitted to a Gaussian $\psi_i(x) \propto e^{-3.8r^2/\mathrm{fm}^2}$. This leads immediately to the following parametrization of the J/ψ's Wigner distribution's (here the constant is in fm^{-2}) :

$$W_{J/\psi}(x,p) = \frac{1}{\pi^3}\exp(-7.6r^2 - p^2/7.6) \tag{3}$$

Many properties for the Wigner transform so defined may be discussed but for our purposes here we should note that

$$\int W_\psi(x,p)dp = |\psi(x)|^2 \tag{4}$$

and for another wavefunction $\chi(x)$'s Wigner transform $W_\chi(x,p)$

$$\int W_\psi(x,p)W_\chi(x,p)dxdy \;\; = \tfrac{1}{(2\pi)^3}|\langle\psi|\chi\rangle|^2, \tag{5}$$

because this is what we need to properly normalize our distributions and to compute overlaps.

So, for our phase-space distribution at any given time $f(\boldsymbol{x},\boldsymbol{p},\tau)$, we model

our probability of pair being measured in the J/ψ-state as

$$P_{J/\psi}(\tau) = (2\pi)^3 \int f(\mathbf{x}, \mathbf{p}, \tau) W_{J/\psi}(\mathbf{x}, \mathbf{p}) d^3x d^3p. \tag{6}$$

We project the pairs onto the J/ψ-state not only at the onset of the calculation, but also throughout the time evolution, monitoring in this way the probability of J/ψ production.

Later on we switched to the "energy projection method", which is ultimately used for projection into $\chi, \psi^{'}$ states as well as into J/ψ . It is based on the distribution over $\bar{c}c$ energy, in the pair rest frame, calculated with the (zero temperature) Cornell potential. One projection, used in Figure 9, is to all bound states, defined by

$$E_{CM} = V_{Cornell}(r) + \frac{p_{rel}^2}{M_c} < 0.88 \text{ GeV}. \tag{7}$$

Later on, we differentiate between various charmonium states again by examining the $\bar{c}c$ pair's energy in its rest frame, and comparing it with the energies of solutions to Schrödinger's equation using the Cornell potential. For example, the lowest s-state solution, using the charm quark mass, has energy $E = 0.33$ GeV, therefore we count all $\bar{c}c$ pairs in our simulation with energy below 0.33 GeV as existing in the J/ψ state.

Classical vs. Quantum Dynamics

In this work, the phase-space distributions of $\bar{c}c$ pairs were evolved in time according to the Fokker-Planck/Langevin equations, which describe nonequilibrium evolution of phase-space distributions during the QGP era. After it is finished and the medium returns to the hadronic phase, our classical distribution $f(\boldsymbol{x}, \boldsymbol{p}, t)$ has to be projected into charmonium quantum states.

He we examine how classical and quantum dynamics correspond to each other in equilibrium, when both are easily available. We simplify by examining the thermal distributions for a Coulombic system, with $V \sim 1/r$. One can

calculate the density of states for the classical system:

$$\begin{aligned} Z &= \int dr dp (4\pi)^2 r^2 p^2 \exp(-(p^2/2\mu - e^2/r)/T) \\ &= \int dE \int dr dp (4\pi)^2 r^2 p^2 \exp(-E/T)\delta(E - p^2/2\mu + 1/r) \\ &= \int dE \exp(-E/T) \int_{max(0,\sqrt{2\mu E}}^{\infty} dp \frac{e^2 p^2}{(p^2/2\mu - E)^4} \end{aligned}$$

As one can see, this integral is divergent for $E > 0$. This means that this distribution is not normalizable and in thermal equilibrium all pairs are ionized. For $E < 0$, we see from examining the partition function

$$\rho(E) \propto (-E)^{-5/2} \tag{8}$$

Now we calculate the quantum mechanical density of states for $E < 0$,

$$\rho(E) = \Sigma_{n=1}^{\infty} n^2 \delta(E + \frac{C}{n^2}) \tag{9}$$

which can be approximated by considering an integral:

$$\begin{aligned} \int_{-\infty}^{E} dE' \rho(E') &= \Sigma_{i=1}^{\infty} i^2 \theta(E + \frac{C}{i^2}) \\ &\sim E^{-3/2} \text{ for large enough E} \end{aligned}$$

Thus, $\rho(E) \sim E^{-5/2}$ for E close to zero: therefore for highly excited states the correspondence principle holds and the classical thermal distribution is recovered. However, classical density of states is not so good of an approximation to the quantum-mechanical density of states for the lowest bound state.

We also tested whether Langevin simulations leads to the correct classical density of states, after some relaxation time. The result of evolving an ensemble of $\bar{c}c$ pairs at a fixed temperature according to classical Langevin dynamics shown in Fig.1 shows that equilibrium is indeed obtained.

Canonical ensembles for N $\bar{c}c$ -pair systems

In this section we will determine a partition function for a canonical ensemble of N charm pair systems (that is, an ensemble of very many systems, where each system contains N $\bar{c}c$ pairs) which correctly averages over different possible pairings of charm and anticharm quarks and can therefore describe recom-

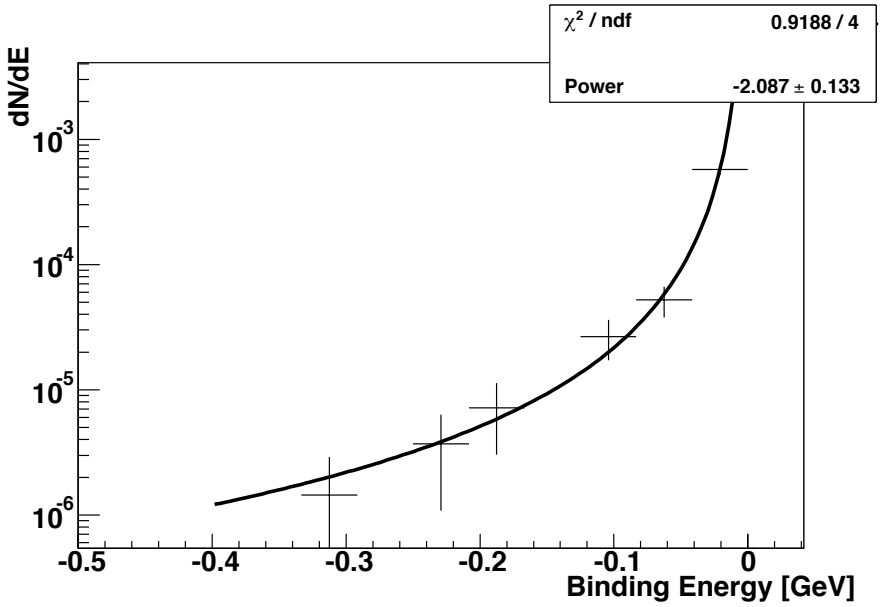

Figure 1: The points show the density of states for an ensemble of $\bar{c}c$ pairs at a fixed temperature $T = 1.5T_c$ obtained by long-time Langevin evolution, compared to a fit with power 2.1 (curve), close to classical nonrelativistic thermal distribution.

bination in heavy-ion collisions. This averaging is possible computationally but is non-trivial, and for RHIC collisions we will take a binary approximation which makes this averaging much easier. We argue, however, that the unsimplified approach is necessary for describing collisions at the Large Hadron Collider, and for this reason we include this discussion here.

Our simulation could be thought of as a canonical ensemble description of charmonium in plasma: we can think of our large set of $\bar{c}c$ pairs as a set of systems, each system containing N pairs, with each system's dynamics modeled as a stochastic interaction with the medium, with a deterministic interaction of each heavy quark with the other quark in the pair. Each system in this set samples the distribution of $\bar{c}c$ pairs in the initial collision, the geometry of the collision, and also samples the stochastic forces on the heavy quarks. Up to this point, we have only thought of each system of this set as consisting of a single $\bar{c}c$ pair. The interaction of charm quarks from different hard events is negligible compared with the stochastic interaction and the interaction within the pair, partly because near T_c, the dynamics of charm pairs seems best described with some generalization of the Lund string model, which allows no interaction between unpaired charm quarks [33]. Therefore, it is simple bookkeeping to think now of the systems as each consisting of N $\bar{c}c$ pairs.

However, even though the dynamics of the system is not changed when considering many $\bar{c}c$ pairs per collision, the hadronization ("pairing") of these $2N$ charm quarks is now a non-trivial issue. For simplicity, assume that the quarks all reach the freezeout temperature T_c at the same proper time. There are $N!$ different possible pairings of the quarks and anti-quarks into charmonium states (each pairing is an element of the permutation group S_N). Call a given pairing σ (which is an element of S_N). Near T_c, the relative energetics of a pairing σ is given by

$$E_i = \sum_i V(|\boldsymbol{r}_i - \boldsymbol{r}'_{\sigma(i)}|), \tag{10}$$

where $V(r)$ is the zero-temperature Cornell potential (with some maximum value at large r, corresponding to the string splitting), $\boldsymbol{r}_i$ the position of the i-th charm quark, $\boldsymbol{r}'$ the position of the i-th charm antiquark, and $\sigma(i)$ the integer in the i-th term of the permutation.

One way to proceed is to average over these pairings according to their Boltzmann factors. In this way, the probability of a given pairing would be given by

$$P(i) = \frac{1}{\mathcal{Z}} \exp(-E_i/T_c),\ \mathcal{Z} = \sum_{i=1}^{N!} \exp(-E_i/T_c). \tag{11}$$

However, this averaging ignores the possibility of survival of bound $\bar{c}c$ states from the start to the finish of the simulation, in that pairings which artificially "break up" bound states are included in the average. This goes against the main point of our last paper: that it is actually the incomplete thermalization of $\bar{c}c$ pairs which explains the survival of charmonium states.

For this reason, the averaging we perform rejects permutations which break up pairs that would otherwise be bound: we average over a subgroup $S_N^{'}$ of S_N, and determine the probability based on this modified partition function:

$$P(i) = \frac{1}{\mathcal{Z}} \exp(-E_i/T_c),\ \mathcal{Z} = \sum_{\sigma \in S_N^{'}} \exp(-E_i/T_c), \tag{12}$$

where E_i specifies the energy of a pairing we permit. We will average over the permutations in this way.

By doing this, we will use a fully canonical ensemble description for charm in plasma, which holds for any value for N, large or small. Previous work in statistical hadronization used the grand canonical approach to explain relative abundances of open and hidden charm [58], which can only be applied where thermalization may be assumed to be complete.